

ITERATIVE RECEIVERS FOR OFDM SYSTEMS WITH DISPERSIVE FADING
AND FREQUENCY OFFSET

A Thesis

by

HUI LIU

Submitted to the Office of Graduate Studies of
Texas A&M University
in partial fulfillment of the requirements for the degree of
MASTER OF SCIENCE

May 2003

Major Subject: Electrical Engineering

ITERATIVE RECEIVERS FOR OFDM SYSTEMS WITH DISPERSIVE FADING
AND FREQUENCY OFFSET

A Thesis

by

HUI LIU

Submitted to Texas A&M University
in partial fulfillment of the requirements
for the degree of

MASTER OF SCIENCE

Approved as to style and content by:

Xiaodong Wang
(Co-Chair of Committee)

Zixiang Xiong
(Co-Chair of Committee)

Erchin Serpedin
(Member)

Garng M.Huang
(Member)

Jyh-Charn(Steve) Liu
(Member)

Chanan Singh
(Head of Department)

May 2003

Major Subject: Electrical Engineering

ABSTRACT

Iterative Receivers for OFDM Systems with Dispersive Fading and Frequency
Offset. (May 2003)

Hui Liu, B.S., Tsinghua University

Co-Chairs of Advisory Committee: Dr. Xiaodong Wang
Dr. Zixiang Xiong

The presence of dispersive fading and inter-carrier interference (ICI) constitute the major impediment to reliable communications in orthogonal frequency-division multiplexing (OFDM) systems. Recently iterative (“Turbo”) processing techniques, which have been successfully applied to many detection/decoding problems, have received considerable attention. In this thesis, we first aim on the design of iterative receiver for single antenna OFDM system with frequency offset and dispersive fading. Further work is then extended to space-time block coded (STBC) OFDM system. At last, the technique is applied to STBC-OFDM system through a newly built channel model, which is based on a physical description of the propagation environment. The performance of such systems are verified by computer simulations. The simulation results show that the iterative techniques work well in OFDM systems.

To My dear family

ACKNOWLEDGMENTS

I would like to thank my advisor, Dr. Xiaodong Wang, for his continuous guidance, support and encouragement throughout my thesis work. I am also thankful to my co-chair, Dr. Zixiang Xiong, my committee members Dr. Garng M.Huang, Dr. Erchin Serpedin, and Dr. Jyh-Charn(Steve) Liu for their valuable comments and time.

I wish to recognize all my colleagues in the Wireless Communication Lab of Texas A&M University, especially Dr. Zhongmin Liu, Dr. Ben Lu, Dr. Zigang Yang, Dr. Yu Zhang, Yan Wang, Yongzhe Xie and Jun Zheng, for the encouragement and insightful discussions.

TABLE OF CONTENTS

CHAPTER		Page
I	INTRODUCTION	1
II	OFDM SYSTEM AND CARRIER FREQUENCY OFFSET	3
	A. OFDM System Model	3
	B. OFDM System with Carrier Frequency Offset	6
	C. Simulation Results	6
III	INTRODUCTION TO CHANNEL MODEL	8
	A. Rayleigh Fading Channels	8
	B. Simulating Fading Channels	11
	C. Simulation Results	12
IV	ITERATIVE RECEIVER FOR OFDM SYSTEM	14
	A. The System Model	15
	B. Receiver Structure	15
	1. SISO Demodulator	17
	2. Channel Estimation Based on EM Algorithm	19
	3. Carrier Frequency Offset Estimation	21
	C. Simulation Results	23
V	ITERATIVE RECEIVER FOR STBC-OFDM SYSTEM	30
	A. The System Model	31
	1. STBC Encoding Algorithm	31
	2. STBC-OFDM System Model	32
	B. Receiver Structure	34
	1. SISO STBC Decoder	35
	2. Carrier Frequency Offset Estimation	38
	C. Simulation Results	41
VI	APPLICATION OF THE PROPOSED ITERATIVE RE- CEIVER FOR NEW BROAD-BAND MIMO FADING CHAN- NEL MODEL	48
	A. Broad-Band MIMO Fading Channel Model	48

CHAPTER	Page
1. Channel Model	48
2. Fading Statistics	50
B. Simulation Results	51
VII CONCLUSIONS	63
REFERENCES	64
VITA	68

LIST OF FIGURES

FIGURE	Page
1	Block diagram of OFDM system. 3
2	ICI effects on the amplitude of the desired signal X_k 7
3	ICI effects on BER in a coded OFDM system with normalized frequency offset $\epsilon = 0.0, 0.1, 0.2$, respectively. Perfect CSI is assumed at the receiver. 7
4	Flat fading channel model. 9
5	Tapped delay model for frequency selective fading channel. 10
6	Power spectral density of the desired fading process. 12
7	Fading channel simulator, $f_d=50\text{Hz}$, $T_s=0.1\text{ms}$ 13
8	Fading channel simulator, $f_d=200\text{Hz}$, $T_s=0.1\text{ms}$ 13
9	A coded OFDM system with iterative receiver. 16
10	BER in a coded OFDM system through a 4-tap frequency selective fading channel with Doppler shift $f_d = 50\text{Hz}$. Carrier frequency offset $f_\epsilon = 0.05/N$ 25
11	BER in a coded OFDM system through a 4-tap frequency selective fading channel with Doppler shift $f_d = 50\text{Hz}$. Carrier frequency offset $f_\epsilon = 0.1/N$ 26
12	BER in a coded OFDM system through a 4-tap frequency selective fading channel with Doppler shift $f_d = 50\text{Hz}$. Carrier frequency offset $f_\epsilon = 0.2/N$ 27
13	BER in a coded OFDM system through a 4-tap frequency selective fading channel with Doppler shift $f_d = 200\text{Hz}$. Carrier frequency offset $f_\epsilon = 0.1/N$ 28

FIGURE	Page
14	BER in a coded OFDM system through a 4-tap frequency selective fading channel with Doppler shift $f_d = 200\text{Hz}$. Carrier frequency offset $f_\epsilon = 0.2/N$ 29
15	A data burst. 33
16	A coded STBC-OFDM system with iterative receiver. 34
17	BER in a coded STBC-OFDM system through a 4-tap frequency selective fading channel with Doppler shift $f_d = 50\text{Hz}$ 42
18	BER in a coded STBC-OFDM system through a 4-tap frequency selective fading channel with Doppler shift $f_d = 200\text{Hz}$ 43
19	BER in a coded STBC-OFDM system through a 4-tap frequency selective fading channel with Doppler shift $f_d = 50\text{Hz}$. Carrier frequency offset $f_\epsilon = 0.1/N$ 44
20	BER in a coded STBC-OFDM system through a 4-tap frequency selective fading channel with Doppler shift $f_d = 200\text{Hz}$. Carrier frequency offset $f_\epsilon = 0.1/N$ 45
21	BER in a coded STBC-OFDM system through a 4-tap frequency selective fading channel with Doppler shift $f_d = 50\text{Hz}$. Carrier frequency offset $f_\epsilon = 0.2/N$ 46
22	BER in a coded STBC-OFDM system through a 4-tap frequency selective fading channel with Doppler shift $f_d = 200\text{Hz}$. Carrier frequency offset $f_\epsilon = 0.2/N$ 47
23	Schematic representation of the MIMO delay spread channel composed of multiple clustered paths. Each path cluster has a mean angle of arrival $\bar{\theta}_l$ and an angle spread δ_l . The absolute antenna spacing is denoted by d 49
24	A coded STBC-OFDM system through broad-band correlated MIMO channels. We assumed a total angle spread of 90 degrees and the cluster angle spread $\sigma_{\theta_l} = 0$ ($l = 0, 1, \dots, 3$). Doppler shift $f_d = 50\text{Hz}$ 53

FIGURE	Page
25	A coded STBC-OFDM system through broad-band correlated MIMO channels. Doppler shift $f_d = 200\text{Hz}$. We assumed a total angle spread of 90 degrees and the cluster angle spread $\sigma_{\theta_l} = 0$ ($l = 0, 1, \dots, 3$). 54
26	A coded STBC-OFDM system through broad-band correlated MIMO channels. We assumed a total angle spread of 90 degrees and the cluster angle spread $\sigma_{\theta_l} = 0.25$ ($l = 0, 1, \dots, 3$). Doppler shift $f_d = 50\text{Hz}$ 55
27	A coded STBC-OFDM system through broad-band correlated MIMO channels. We assumed a total angle spread of 90 degrees and the cluster angle spread $\sigma_{\theta_l} = 0.25$ ($l = 0, 1, \dots, 3$). Doppler shift $f_d = 200\text{Hz}$ 56
28	A coded STBC-OFDM system through broad-band correlated MIMO channels. We assumed a total angle spread of 90 degrees and the cluster angle spread $\sigma_{\theta_l} = 1$ ($l = 0, 1, \dots, 3$). Doppler shift $f_d = 50\text{Hz}$ 57
29	A coded STBC-OFDM system through broad-band correlated MIMO channels. We assumed a total angle spread of 90 degrees and the cluster angle spread $\sigma_{\theta_l} = 1$ ($l = 0, 1, \dots, 3$). Doppler shift $f_d = 200\text{Hz}$ 58
30	A coded STBC-OFDM system through broad-band correlated MIMO channels. We assumed a total angle spread of 90 degrees and the cluster angle spread $\sigma_{\theta_l} = 0$ ($l = 0, 1, \dots, 3$). Doppler shift $f_d = 50\text{Hz}$. Frequency offset $f_\epsilon = 0.1/N$ 59
31	A coded STBC-OFDM system through broad-band correlated MIMO channels. We assumed a total angle spread of 90 degrees and the cluster angle spread $\sigma_{\theta_l} = 0.25$ ($l = 0, 1, \dots, 3$). Doppler shift $f_d = 50\text{Hz}$. Frequency offset $f_\epsilon = 0.1/N$ 60
32	A coded STBC-OFDM system through broad-band correlated MIMO channels. We assumed a total angle spread of 90 degrees and the cluster angle spread $\sigma_{\theta_l} = 1$ ($l = 0, 1, \dots, 3$). Doppler shift $f_d = 50\text{Hz}$. Frequency offset $f_\epsilon = 0.1/N$ 61

FIGURE	Page
33	A coded STBC-OFDM system through broad-band correlated MIMO channels. We assumed a total angle spread of 90 degrees and the cluster angle spread $\sigma_{\theta_l} = 1$ ($l = 0, 1, \dots, 3$). Doppler shift $f_d = 200\text{Hz}$. Frequency offset $f_\epsilon = 0.1/N$ 62

CHAPTER I

INTRODUCTION

Orthogonal frequency-division multiplexing (OFDM) has received increasing attention in wireless broadcasting systems for its ability of supporting high data-rate communications. While inherently robust against multi-path fading, OFDM has been shown to be very sensitive to frequency offset [1], [2], [3], [4], [5]. A carrier offset can destroy sub-carrier orthogonality, thus can introduce inter-carrier interference (ICI) and seriously degrade system performance. In addition to frequency offset [10], the frequency-selective fading channel state information is also unknown to the receiver. So efficient and accurate estimation of frequency offset and channel state information is very crucial to an OFDM system.

Recently iterative (“Turbo”) processing techniques [6], [8], [10], [11] have also received considerable attention. The so-called Turbo-principle can be successfully applied to many detection/decoding problems such as serial concatenated decoding, equalization, coded modulation and joint source and channel decoding. Compared with previous non-iterative receivers, iterative receivers can successively improve receiver performance in typical wireless channels with very fast fading, at a reasonable computational complexity well suited for real-time implementations.

Further work can be extended to space-time block coded (STBC) OFDM systems [11], [12], [13] and correlated MIMO channel models [22], [23], [24]. Transmit diversity and space-time coding [14], [15], [16], [17] have been proposed as a means to combat multi-path fading. For a fixed number of transmit antennas, its decoding complexity increases exponentially with the transmission rate. Since space-time

The journal model is *IEEE Transactions on Automatic Control*.

codes are originally designed for flat-fading channels, it is challenging to apply them over multi-path fading channels. One approach [12] is to employ OFDM which convert a multi-path channel into parallel independent frequency-flat sub-channels. In STBC-OFDM, channel state information between each transmit and receive antenna pair is required for coherent decoding. However, for each OFDM tone, since the received signals are a superposition of signals transmitted from different antennas, the simple techniques [10], [19] used in single antenna cases cannot be easily applied. Furthermore, STBC-OFDM systems still suffer from severe performance degradation due to frequency offset. Therefore, the proposed iterative receiver structure also aids in channel and frequency offset estimation.

In this thesis, we first aim on the design of iterative receiver for single antenna OFDM system with frequency offset and frequency-selective fading. Further work is then extended to space-time block coded (STBC) OFDM system. At last, the technique is applied to STBC-OFDM system through a newly built channel model, which is based on a physical description of the propagation environment. The performance of such systems are verified by computer simulations and the simulation results are given.

CHAPTER II

OFDM SYSTEM AND CARRIER FREQUENCY OFFSET

Orthogonal frequency division multiplexing (OFDM), which can transform a frequency-selective fading channel into many parallel flat fading sub-channels, is an efficient technique to combat multi-path delay spread in high-rate wireless systems. It is, however, very sensitive to carrier frequency offset (CFO), which is caused by misalignment in carrier frequencies or Doppler shift.

In this chapter, we will first introduce the structure of a basic OFDM system. Then inter-carrier interference (ICI), which is caused by CFO, will be studied.

A. OFDM System Model

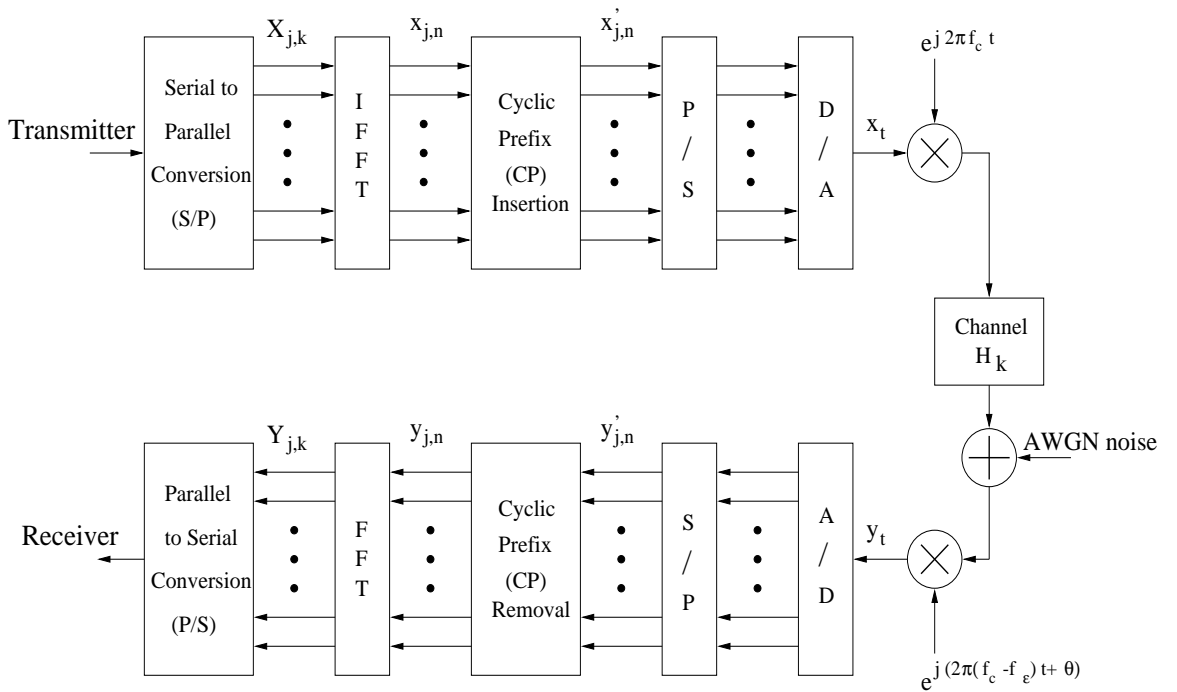


Fig. 1. Block diagram of OFDM system.

In an OFDM system, the available bandwidth is partitioned into N sub-channels thus the symbol duration is N times of that of the single carrier system with the same symbol rate. This significantly reduces normalized delay spread hence is more robust to time dispersive wireless channel.

In discrete Fourier transform (DFT) based OFDM systems, IDFT is used in the transmitter to achieve orthogonality among sub-carriers which allows a simple DFT based receiver structure. A cyclic prefix (CP) consisting of the last N_g samples of the output of the IDFT block is inserted in front of each OFDM system symbol. The time length of the CP should be greater than the length of the discrete-time baseband channel impulse response, i.e. $N_g \geq L$, where L is the number of the resolvable paths of the channel, in order to combat with the inter-symbol interference (ISI). If only P out of N sub-carriers are used to modulate information symbols, the $N - P$ unused sub-carriers are often referred to as the virtual carriers. Then the samples are applied to a pair of D/A converters, and the analog I and Q signals are up-converted to RF. The modulated signal is transmitted over the channel, received and down-converted to baseband. After the baseband signal is digitalized by the A/D converters, the CP interval is removed, which makes the received sequence the circular convolution of the transmitted sequence with the channel impulse response $\{h(l)\}_{l=0}^{L-1}$. Then the signal is demodulated using a DFT on a block of N samples.

The general transmitter and receiver format for an OFDM system is shown in Fig.1. An IDFT/DFT pair is used as the OFDM modulator/demodulator. The N point IDFT output sequence for the j th OFDM symbol is given by

$$x_{j,n} = \frac{1}{N} \sum_{k=0}^{N-1} X_{j,k} e^{j \frac{2\pi k}{N} n}, \quad n = 0, 1, \dots, N - 1 \quad (2.1)$$

If we model the time-domain channel impulse response as tapped delay line, i.e.

$$h_t = \sum_{l=0}^{L-1} h(l) \delta\left(t - \frac{l}{W}\right), \quad (2.2)$$

with W being the bandwidth of the transmitted signal, then the received time-domain digitalized baseband sequence $y'_j \triangleq \{y'_{j,0}, y'_{j,1}, \dots, y'_{j,N+N_g-1}\}$ can be written as

$$y'_j = x'_j \star h + n'_j, \quad (2.3)$$

where $x'_j \triangleq \{x'_{j,0}, x'_{j,1}, \dots, x'_{j,N+N_g-1}\}$, is the transmitted time-domain digitalized baseband sequence, $h \triangleq \{h(0), h(1), \dots, h(L-1)\}$, is the time-domain channel impulse response sequence, and n'_j is the corresponding noise sequence. \star denotes linear convolution. When the cyclic prefix is properly inserted, this linear convolution is equivalent to the circular convolution within the concerned time interval $[N_g, N+N_g-1]$, namely

$$y_j = x_j \otimes h + n_j, \quad (2.4)$$

with \otimes representing circular convolution, and x_j/y_j being the transmitted/received sequence without cyclic prefix. According to the discrete time linear system theory, circular convolution in time domain is equivalent to multiplication in frequency domain, thus we get

$$Y_{j,k} = X_{j,k} \cdot H_k + N_{j,k}, \quad k = 0, 1, \dots, N-1 \quad (2.5)$$

where $\{X_{j,k}\}_{k=0}^{N-1} = \text{DFT}_N\{x_j\}$, $\{Y_{j,k}\}_{k=0}^{N-1} = \text{DFT}_N\{y_j\}$, and $\{H_k\}_{k=0}^{N-1} = \text{DFT}_N\{h\}$.

B. OFDM System with Carrier Frequency Offset

If there is a small frequency offset f_ϵ between the transmit and receive oscillators, the received sequence in time domain can be expressed as

$$y_n = \frac{1}{N} \sum_{k=0}^{N-1} X_k \cdot H_k e^{j \frac{2\pi(k+\epsilon)}{N} n} + \omega_n, \quad n = 0, 1, \dots, N-1. \quad (2.6)$$

where $\epsilon \triangleq f_\epsilon N$ is the normalized carrier frequency offset, and ω_n is Gaussian white noise. Notice we dropped the subscript 'j' for the sake of simplicity. After DFT is implemented to the received sequence $\{y_n\}_{n=0}^{N-1}$, we get

$$\begin{aligned} Y_k &= \sum_{n=0}^{N-1} y_n e^{-j \frac{2\pi n}{N} k} \quad k = 0, 1, \dots, N-1 \\ &= \frac{1}{N} \sum_{l=0}^{N-1} X_l \cdot H_l \sum_{n=0}^{N-1} e^{j \frac{2\pi n}{N} (l-k+\epsilon)} + \Omega_k. \end{aligned}$$

Define $S(l-k) = \frac{1}{N} \sum_{n=0}^{N-1} e^{j \frac{2\pi n}{N} (l-k+\epsilon)}$, then

- $l = k$ $S(0) = \frac{\sin(\pi\epsilon)}{N \sin(\frac{\pi\epsilon}{N})} \cdot e^{j\pi\epsilon \frac{N-1}{N}}$
- $l \neq k$ $S(l-k) = \frac{\sin(\pi\epsilon)}{N \sin(\frac{\pi(l-k+\epsilon)}{N})} \cdot e^{j\pi\epsilon \frac{N-1}{N}} e^{-j\pi \frac{l-k}{N}}$.

Thus Y_k can be re-written as

$$Y_K = X_k \cdot H_k \cdot S(0) + \sum_{l=0, l \neq k}^{N-1} X_l \cdot H_l \cdot S(l-k) + \Omega_k, \quad k = 0, 1, \dots, N-1. \quad (2.7)$$

C. Simulation Results

As can be seen from Eq.2.7 and Fig.2, all X_l 's, $l \neq k$, have ICI effects on the desired signal X_k . In Fig.3, we simulated the effect of frequency offset on the BER of a coded OFDM system with $N = 128$. One can see from Fig.3 that even a small amount of f_ϵ can severely degrade system performance.

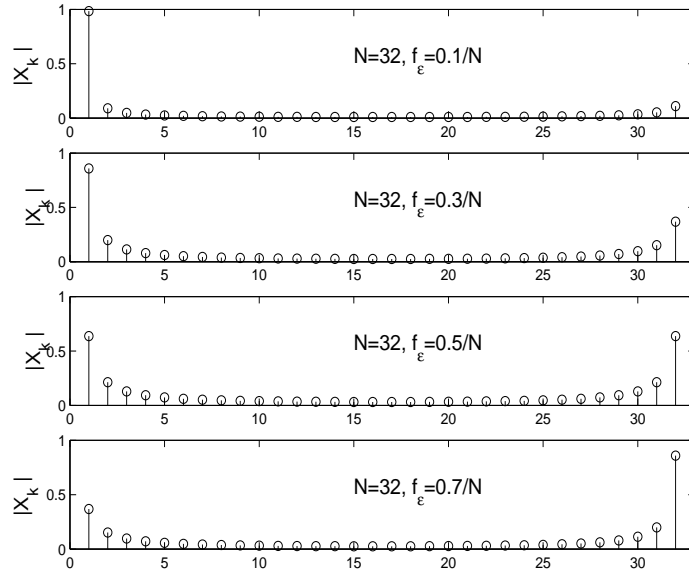


Fig. 2. ICI effects on the amplitude of the desired signal X_k .

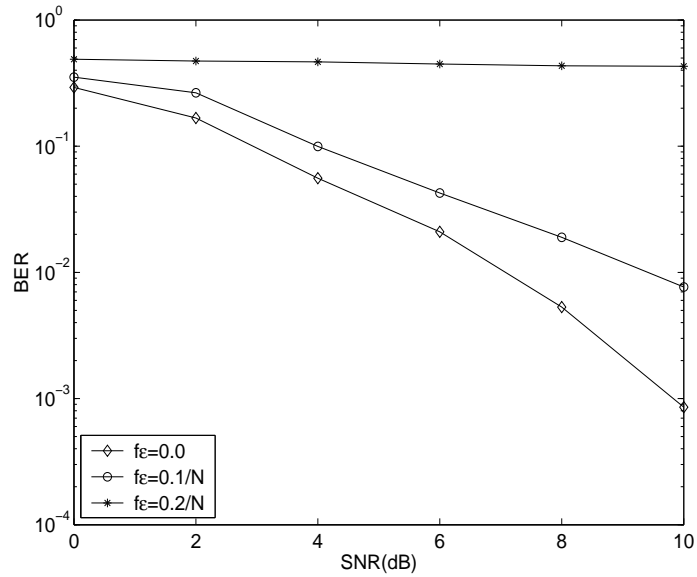


Fig. 3. ICI effects on BER in a coded OFDM system with normalized frequency offset $\epsilon = 0.0, 0.1, 0.2$, respectively. Perfect CSI is assumed at the receiver.

CHAPTER III

INTRODUCTION TO CHANNEL MODEL

In this chapter, a brief introduction of Rayleigh fading channel model and the corresponding channel simulator will be given. We will be using this channel model in the subsequent chapters.

A. Rayleigh Fading Channels

Fading is used to describe the rapid fluctuation of the amplitude of a radio signal over a short period of time or travel distance. It is caused by interference between two or more versions of the transmitted signal which arrive at the receiver at slightly different times. These multi-path waves combine at the receiver antenna to give a resultant signal which can vary widely in amplitude and phase, depending on the distribution of the intensity and relative propagation time of the waves and the bandwidth of the transmitted signal [7]. Suppose the transmitted signal has a complex envelope $g_s(t)$. The received signal can be modeled as

$$g_r(t) = \sum_k \rho_k e^{j\theta_k} g_s(t - \tau_k) + N(t), \quad (3.1)$$

where ρ_k = attenuation of the k^{th} path,

θ_k = phase shift of the k^{th} path,

τ_k = delay of the k^{th} path,

$N(t)$ = Gaussian white noise.

Define τ_m to be the maximum delay difference between any two significant paths. If $\tau_m \sim T_s$, the various delayed paths will cause ISI.

We first consider the case where $\tau_m \ll T_s$. The model in (3.1) can be simplified

to

$$\begin{aligned} g_r(t) &= g_s(t) \sum k \rho_k e^{j\theta_k} + N(t) \\ &\triangleq h g_s(t) + N(t) \end{aligned} \quad (3.2)$$

Where $h \triangleq x + jy \triangleq a e^{j\phi} \triangleq \sum_k \rho_k e^{j\theta_k}$ is a zero-mean, complex Gaussian random variable with

$$\begin{aligned} f_{x,y}(x, y) &= \frac{1}{2\pi\sigma^2} \exp\left(-\frac{x^2 + y^2}{2\sigma^2}\right), \\ f_a(a) &= \frac{a}{\sigma^2} \exp\left(-\frac{a^2}{2\sigma^2}\right) U(a), \\ f_\phi(\phi) &= \frac{1}{2\pi}, \quad 0 \leq \phi \leq 2\pi. \end{aligned} \quad (3.3)$$

The above approximation is valid under the assumptions that the number of paths is large, and no one path has substantially smaller attenuation than all the others, then the central limit theorem can be applied to both x and y and they can be well approximated as Gaussian random variables. This is known as *Rayleigh flat fading* channel which can be modeled by Fig.4.

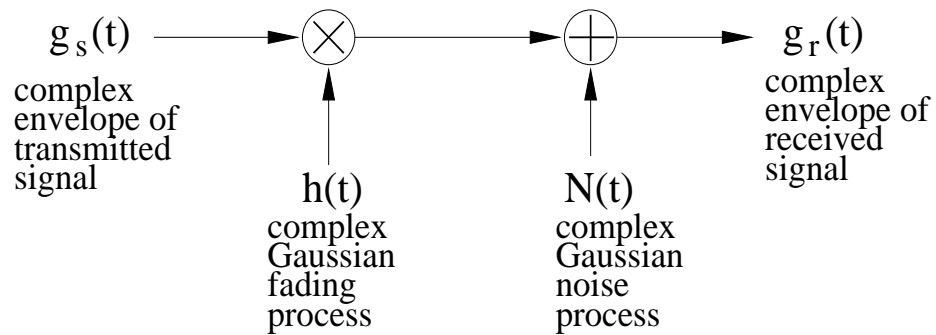


Fig. 4. Flat fading channel model.

If $\tau_m \sim T_s$ or $\tau_m > T_s$, the channel will distort (filter) the signal rather than just attenuate the signal, resulting in what is known as a *frequency selective fading*

channel. The channel can be modeled as a tapped delay line, as pictured in Fig.5.

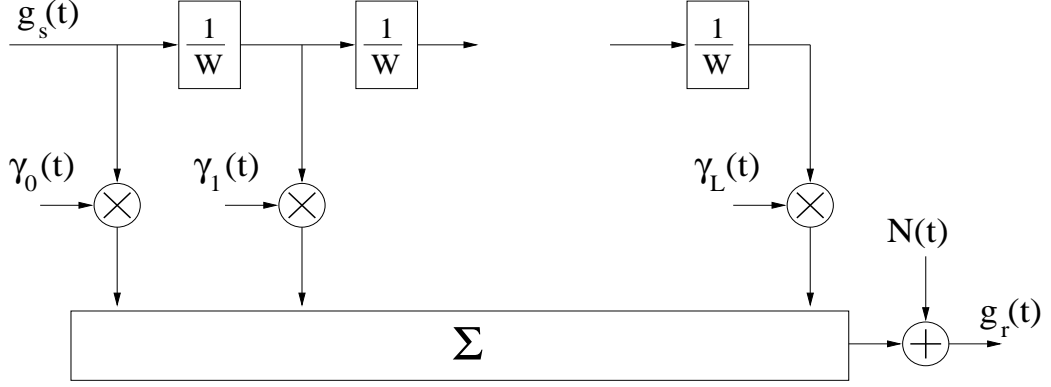


Fig. 5. Tapped delay model for frequency selective fading channel.

$$g_r(t) = \sum_{n=0}^{L-1} \gamma_n g_s\left(t - \frac{n}{W}\right) + N(t) \quad (3.4)$$

where W is the bandwidth of the transmitted signal, and $L \cong W\tau_m$ represents the number of resolvable paths. Each γ_n can be viewed as individual flat fading process as described before.

If either the transmitter or receiver is in motion, the received signal will be shifted in frequency relative to the transmitted frequency, known as Doppler spread, which induces time selective fading. Let f_d denote the maximum Doppler shift, then

$$f_d = \frac{v}{c} f_c, \quad (3.5)$$

where v = velocity of mobile,

c = speed of light,

f_c = carrier frequency.

The power spectral density (PSD) of the fading process $h(t)$ in Fig.4 and $\gamma_n(t)$ in

Fig.5 is given by

$$H(f) \text{ (or } \Gamma_n(f)) \propto \frac{1}{\sqrt{f_d^2 - (f - f_c)^2}}, \quad (3.6)$$

while the corresponding autocorrelation function is given by

$$R_{h,h}(\tau) \propto J_0(2\pi f_d \tau), \quad (3.7)$$

where $J_0(\cdot)$ denotes the zeroth order Bessel function of the first kind.

B. Simulating Fading Channels

Let $X(t)$ be a realization of a random process over some time interval $[0, T]$. Next produce a periodic signal $\tilde{X}(t)$ by repeating this waveform every T seconds. Since $\tilde{X}(t)$ is periodic, it has a Fourier Series representation

$$\tilde{X}(t) = \sum_k X_k e^{jk\omega_0 t}, \quad \omega_0 = \frac{2\pi}{T}.$$

Furthermore, it has a line spectrum given by

$$S_{\tilde{X}, \tilde{X}}(f) = \sum_k \sigma_k^2 \delta(f - kf_0), \quad \sigma_k^2 = \mathbb{E}\{|X_k|^2\}.$$

The σ_k can be chosen to shape the PSD to any desired form. We want to pick

$$\sigma_k^2 = \frac{\alpha}{\sqrt{f_d^2 - (kf_0)^2}},$$

as described in formula (3.6) and shown in Fig.6. α is chosen such that the random process is normalized to have unit power, i.e.,

$$\mathbb{E}\{|\tilde{X}(t)|^2\} = 1 \quad \implies \quad \sum_k \sigma_k^2 = 1.$$

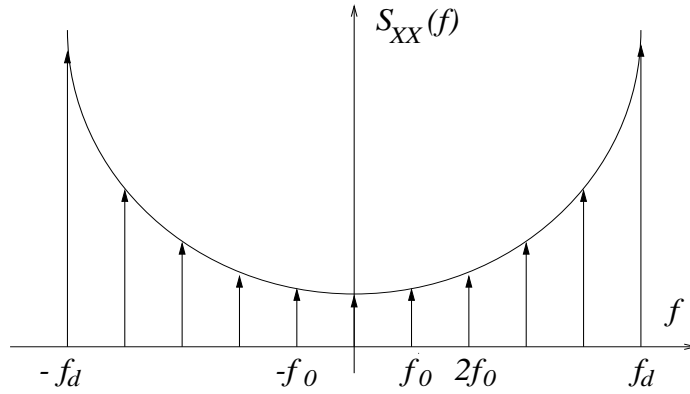


Fig. 6. Power spectral density of the desired fading process.

C. Simulation Results

In this part, we provide computer simulation results of the desired *Rayleigh* fading process. In the simulation, the magnitude, phase, PSD and autocorrelation of the fading process are studied. Fig.7 and Fig.8 are for $f_d=50\text{Hz}$, 200Hz , respectively.

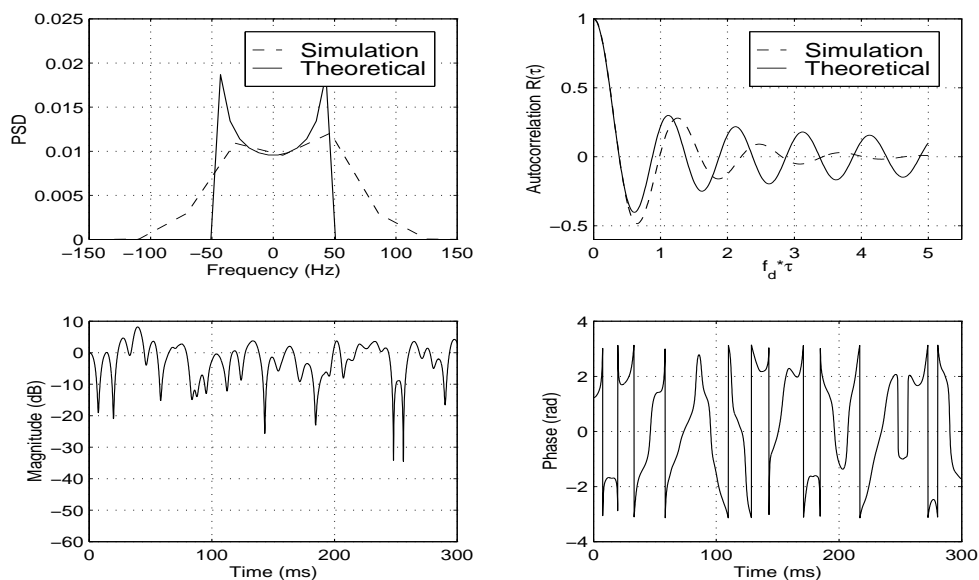


Fig. 7. Fading channel simulator, $f_d=50\text{Hz}$, $T_s=0.1\text{ms}$.

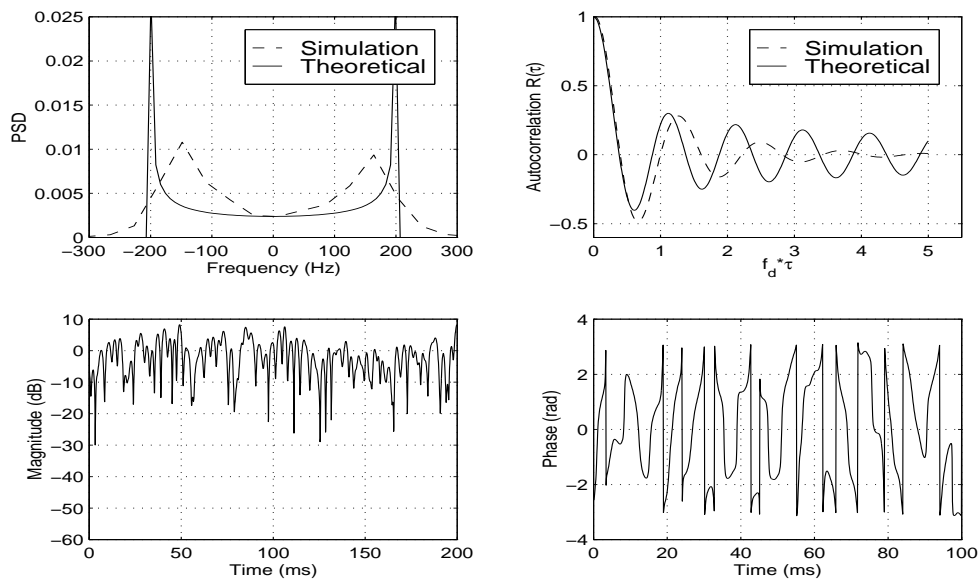


Fig. 8. Fading channel simulator, $f_d=200\text{Hz}$, $T_s=0.1\text{ms}$.

CHAPTER IV

ITERATIVE RECEIVER FOR OFDM SYSTEM

Efficient and accurate channel estimation and frequency offset estimation for OFDM is necessary to coherently demodulate received data. However, estimating a channel that is subject to frequency selective Rayleigh fading is a challenging problem in OFDM systems. EM-based iterative algorithm [19] is an efficient way to estimate the channel impulse response (CIR) of an OFDM system. This algorithm is capable of improving the channel estimate by making use of pilot tones to obtain the initial estimate for iterative steps. On estimating the frequency offset in my work, I will utilize an existing computationally efficient algorithm [5] designed for single antenna OFDM systems. This algorithm combines the conditional maximum likelihood approach and the low-rank property of the narrow-band sub-channels. It also takes advantage of available multiple frames of received data to refine the carrier frequency offset estimation.

Iterative ('Turbo') processing techniques have recently received more and more attention followed by the discovery of the powerful Turbo codes. Similarity in terms of system model can be found between coded CDMA and single user OFDM systems. Therefore, the technique of iterative soft interference cancelation and decoding for coded CDMA [6] can be modified and applied to OFDM systems with inter-channel interference (ICI).

It is very intuitive to combine EM algorithm with the so-called Turbo-principle in the receiver structure for OFDM systems, to achieve successively improved receiver performance. Besides, the computational cost for implementing the EM-based turbo receiver is low and the computation is numerically stable.

A. The System Model

Under the assumption that the fading channel coefficients remain constant during one OFDM symbol interval, an OFDM system with carrier frequency offset can be modeled in terms of vectors and matrices as follows,

$$\underline{Y} = WF(\epsilon)W^I H_F \underline{X} + \underline{\Omega} \quad (4.1)$$

$$\text{where } F(\epsilon) \triangleq \text{diag}\{1, e^{j\frac{2\pi\epsilon}{N}}, \dots, e^{j\frac{2\pi\epsilon(N-1)}{N}}\}$$

$$H_F \triangleq \text{diag}\{\underline{H}\}$$

- ◇ \underline{Y} : $N \times 1$ vector consisting of received signals at N sub-carriers
- ◇ \underline{X} : $N \times 1$ vector consisting of the MPSK symbols transmitted at N sub-carriers
- ◇ \underline{H} : $N \times 1$ vector consisting of fading channel frequency response
- ◇ $\underline{\Omega}$: $N \times 1$ complex Gaussian vector with zero mean and covariance matrix $\sigma^2 I$
- ◇ ϵ : Frequency offset normalized by the OFDM sub-carrier spacing
- ◇ W, W^I : $N \times N$ DFT matrix, iDFT matrix, respectively

B. Receiver Structure

We consider a coded OFDM system with N sub-carriers, signaling through a frequency-selective fading channel in the presence of frequency offset, as shown in Eq.(4.1). We propose a turbo receiver for this system, shown in Fig.9, which iterates between a soft-input soft-output (SISO) demodulator based on soft interference cancellation and linear MMSE filtering, and a SISO channel decoding stage. The two stages are separated by a deinterleaver and an interleaver. The SISO demodulator delivers the a

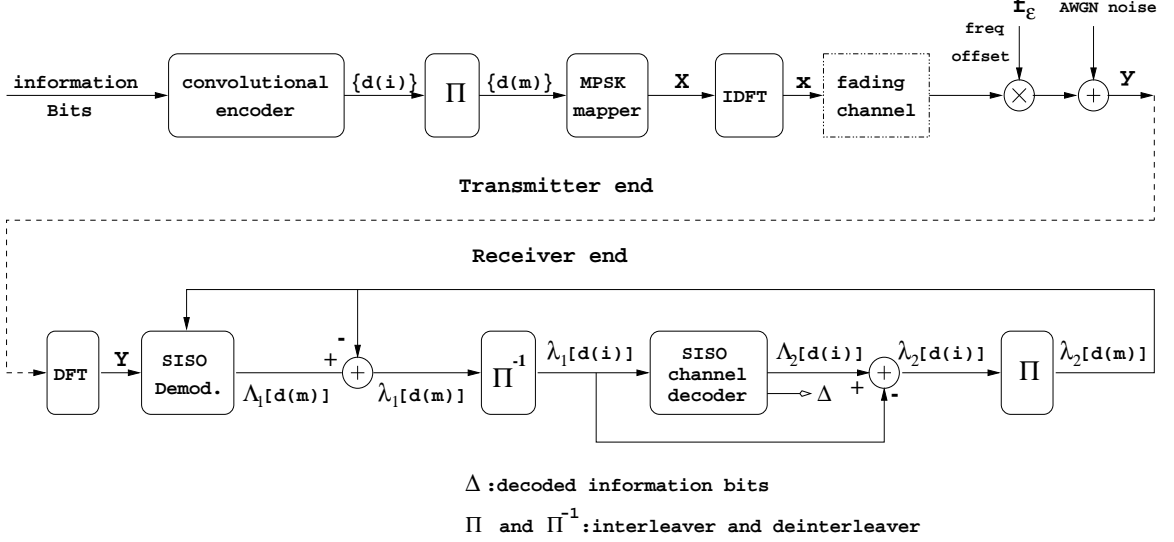


Fig. 9. A coded OFDM system with iterative receiver.

posteriori log-likelihood ratio (LLR) of a transmitted “+1” and a transmitted “-1” for every code bit,

$$\begin{aligned}
 \Lambda_1[d(m)] &\triangleq \log \frac{P[d(m) = +1|\underline{Y}]}{P[d(m) = -1|\underline{Y}]} \\
 &= \underbrace{\log \frac{P[\underline{Y}|d(m) = +1]}{P[\underline{Y}|d(m) = -1]}}_{\lambda_1[d(m)]} + \underbrace{\log \frac{P[d(m) = +1]}{P[d(m) = -1]}}_{\lambda_2^P[d(m)]}
 \end{aligned} \tag{4.2}$$

where the second term in (4.2), represents the *a priori* LLR of the code bit $d(m)$, which is computed by the channel decoder in the previous iteration, interleaved and then fed back to the SISO demodulator. The superscript ^P indicates the quantity obtained from the previous iteration. For the first iteration, assuming equally likely code bits, i.e., no prior information available, we then have $\lambda_2^P[d(m)] = 0$. The first term in (4.2) represents the *extrinsic* information delivered by the SISO demodulator, based on the received signal \underline{Y} , system structure and the prior information about all the code bits. The extrinsic information $\lambda_1[d(m)]$, which is not influenced by the *a priori*

information $\lambda_2^P[d(m)]$ provided by the channel decoder, is then reverse interleaved and fed into the channel decoder, as the *a priori* information in the next iteration.

Based on the prior information $\lambda_1^P[d(i)]$, and the trellis structure of the channel code, the SISO decoder computes the *a posteriori* LLR of each code bit

$$\begin{aligned}\Lambda_2[d(i)] &\triangleq \log \frac{P[d(i) = +1 | \{\lambda_1^P[d(i)]\}; \text{decoding}]}{P[d(i) = -1 | \{\lambda_1^P[d(i)]\}; \text{decoding}]} \\ &= \lambda_2[d(i)] + \lambda_1^P[d(i)].\end{aligned}\quad (4.3)$$

1. SISO Demodulator

1) Soft interference cancelation:

Each complex symbol $X(n)$ can be represented by a J -dim binary bit vector, i.e. $[d(n, 1), \dots, d(n, j), \dots, d(n, J)]^T$, where $J \triangleq \log_2 |\Omega_c|$ and $d(n, j) \in \{+1, -1\}$ denotes the j -th binary bit of the n -th complex code symbol.

$$\begin{aligned}\hat{X}(n) &\triangleq \mathbb{E}\{X(n)\} = \sum_{X_i \in \Omega_c} X_i P[X(n) = X_i], \quad n = 1, 2, \dots, N \\ &= \sum_{X_i \in \Omega_c} X_i \prod_{j=1}^J P[d(n, j) = D(i, j)], \quad D(i, j) \in \{+1, -1\} \\ &= \sum_{X_i \in \Omega_c} X_i \prod_{j=1}^J \frac{\exp\{D(i, j) \lambda_2^P[d(n, j)]\}}{1 + \exp\{D(i, j) \lambda_2^P[d(n, j)]\}}\end{aligned}$$

$$\underline{\hat{X}} \triangleq [\hat{X}(1), \hat{X}(2), \dots, \hat{X}(N)]^T$$

$$\underline{\hat{X}}_n \triangleq \underline{\hat{X}} - \hat{X}(n) \underline{e}_n = [\hat{X}(1), \dots, \hat{X}(n-1), 0, \hat{X}(n+1), \dots, \hat{X}(N)]^T$$

$$\underline{Y}_n \triangleq \underline{Y} - \psi H_F \underline{\hat{X}}_n = \psi H_F (\underline{X} - \underline{\hat{X}}_n) + \Omega$$

where $\psi \triangleq WF(\epsilon)W^T$, $\psi\psi^H = I$

2) Instantaneous linear MMSE filtering:

$$Z(n) = \underline{\omega}_n^H \underline{Y}_n, \quad n = 1, 2, \dots, N$$

where $\underline{\omega}_n \in \mathbb{C}^N$ is chosen to minimize the mean-square error between the transmitted $X(n)$ and the filter output $Z(n)$, i.e.,

$$\begin{aligned} \underline{\omega}_n &= \arg \min_{\underline{\omega}_n \in \mathbb{C}^N} \mathbb{E} \left\{ \left| X(n) - \underline{\omega}_n^H \underline{Y}_n \right|^2 \right\} \\ &= \arg \min_{\underline{\omega}_n \in \mathbb{C}^K} \left\{ \underline{\omega}_n^H \mathbb{E} \{ \underline{Y}_n \underline{Y}_n^H \} \underline{\omega}_n - \underline{\omega}_n^H \mathbb{E} \{ X^*(n) \underline{Y}_n \} - \mathbb{E} \{ X(n) \underline{Y}_n^H \} \underline{\omega}_n \right\} \end{aligned} \quad (4.4)$$

To get $\underline{\omega}_n$, we first take derivative of Eq.(4.4) with respect to $\underline{\omega}_n$. After some manipulations, we have:

$$\begin{aligned} \underline{\omega}_n &= [\mathbb{E} \{ \underline{Y}_n \underline{Y}_n^H \}]^{-1} \mathbb{E} \{ X^*(n) \underline{Y}_n \} \\ \mathbb{E} \{ \underline{Y}_n \underline{Y}_n^H \} &= \psi H_F \text{cov}(\underline{X} - \hat{\underline{X}}_n) H_F^H \psi^H + \sigma^2 I \\ \text{cov}(\underline{X} - \hat{\underline{X}}_n) &= \text{diag} \{ 1 - |\hat{X}(1)|^2, \dots, 1 - |\hat{X}(n-1)|^2, 1, 1 - |\hat{X}(n+1)|^2, \\ &\quad \dots, 1 - |\hat{X}(n)|^2 \} \\ \mathbb{E} \{ X^*(n) \underline{Y}_n \} &= \psi H_F \underline{e}_n \end{aligned}$$

Finally we get:

$$\underline{\omega}_n = \frac{H(n)}{|H(n)|^2 + \sigma^2} \psi \underline{e}_n \quad n = 1, 2, \dots, N. \quad (4.5)$$

Where \underline{e}_n denotes a $N \times 1$ vector of all zeros, except for the n th element, which is 1.

And the corresponding output of the MMSE filter is given by:

$$\begin{aligned} Z(n) &= \frac{H^*(n)}{|H(n)|^2 + \sigma^2} \underline{R}(n) \quad n = 1, 2, \dots, N \\ \text{where } \underline{R}(n) &= W F(\epsilon)^H W^T \underline{Y}(n). \end{aligned} \quad (4.6)$$

3) Gaussian approximation of soft MMSE filter output:

We assume that the output of the soft instantaneous MMSE filter $Z(n)$ represents the output of an equivalent additive Gaussian noise channel having $X(n)$ as its input symbol. This equivalent channel can be represented as:

$$\begin{aligned} Z(n) &= \mu_n X(n) + \eta_n, \\ \text{where } \mu_n &= \text{E}\{Z(n)X^*(n)\} = \frac{|H(n)|^2}{|H(n)|^2 + \sigma^2} \\ v^2(n) &\triangleq \text{Var}\{Z(n)\} = \mu_n - \mu_n^2. \end{aligned}$$

Then the *a posteriori* LLR of $d(n, j)$ at the output of soft demodulator can be computed as follows:

$$\begin{aligned} \Lambda_1[d(n, j)] &\triangleq \log \frac{P[d(n, j) = +1|Y]}{P[d(n, j) = -1|Y]} = \log \frac{P[d(n, j) = +1|\hat{X}(n)]}{P[d(n, j) = -1|\hat{X}(n)]} \\ &= \log \frac{\sum_{X_i \in X_j^+} p[\hat{X}(n)|X(n) = X_i]P[X_i]}{\sum_{X_i \in X_j^-} p[\hat{X}(n)|X(n) = X_i]P[X_i]} \\ &= \log \underbrace{\frac{\sum_{X_i \in X_j^+} \exp\left(-\frac{|\hat{X}(n) - \mu(n)X_i|^2}{v^2(n)} + \sum_{j' \neq j} \frac{D(i, j')}{2} \lambda_2^{\pi \mathbf{P}}[d(n, j')]\right)}{\sum_{X_i \in X_j^-} \exp\left(-\frac{|\hat{X}(n) - \mu(n)X_i|^2}{v^2(n)} + \sum_{j' \neq j} \frac{D(i, j')}{2} \lambda_2^{\pi \mathbf{P}}[d(n, j')]\right)}}_{\lambda_1[d(n, j)]} + \lambda_2^{\pi \mathbf{P}}[d(n, j)] \\ \lambda_2^{\pi \mathbf{P}}[d(n, j)] &\triangleq \log \frac{P[d(n, j) = +1]}{P[d(n, j) = -1]} \quad j = 1, 2, \dots, J \end{aligned}$$

2. Channel Estimation Based on EM Algorithm

The Expectation-Maximization (EM) algorithm is a technique for finding maximum likelihood estimates of system parameters in a broad range of problems where observed data are incomplete. Considering the general OFDM model in frequency domain without carrier frequency offset in Eq.(4.7), note that we will drop the index 'n' for

simplicity in the following derivations.

$$Y(n) = X(n) \cdot H(n) + \Omega(n) \quad n = 0, 1, \dots, N. \quad (4.7)$$

The two-step procedure at the P-th iteration is as follows:

- E – step : $Q(H|H^{(P)}) = E\{\log f(Y, X|H)|Y, H^{(P)}\}$
- M – step : $\tilde{H}^{(P+1)} = \arg \max_H Q(H|H^{(P)})$

For M -PSK constellation,

$$\begin{aligned} f(Y, X_i|H) &= P(X_i) \cdot f(Y|H, X_i) \triangleq P(X_i) \cdot f_i(Y|H) \\ &= P(X_i) \cdot \frac{1}{\sqrt{2\pi}\sigma} \exp\left\{-\frac{1}{2\sigma^2}\|Y - H \cdot X_i\|^2\right\} \quad i = 1, 2, \dots, M, \end{aligned}$$

where $\{X_i\}_{i=1}^M$ is the M -PSK constellation set. $P(\cdot)$ and $f(\cdot)$ denote probability and probability density function, respectively. Then we have in E-step:

$$\begin{aligned} Q(H|H^{(P)}) &= E\{\log f(Y, X|H)|Y, H^{(P)}\} \\ &= \sum_{i=1}^M \log f(Y, X_i|H) \cdot P(X_i|Y, H^{(P)}) \\ &= \sum_{i=1}^M \log f(Y, X_i|H) \cdot \frac{f(Y, X_i|H^{(P)})}{f(Y|H^{(P)})} \\ &= \sum_{i=1}^M \log f(Y, X_i|H) \cdot P(X_i) \cdot \frac{f_i(Y|H^{(P)})}{f(Y|H^{(P)})} \\ &= \sum_{i=1}^M \log [P(X_i) \cdot f_i(Y|H)] \cdot P(X_i) \cdot \frac{f_i(Y|H^{(P)})}{f(Y|H^{(P)})}. \quad (4.8) \end{aligned}$$

In M-step, we want to find H such that $Q(H|H^{(P)})$ in Eq.(4.8) is maximized. By taking derivative of $Q(H|H^{(P)})$ with respect to H and set the derivative to zero, we

get:

$$\tilde{H}^{(P+1)} = \frac{\sum_{i=1}^M X_i^* \cdot Y \cdot P(X_i) \frac{f_i(Y|H^{(P)})}{f(Y|H^{(P)})}}{\sum_{i=1}^M X_i^* \cdot X_i \cdot P(X_i) \frac{f_i(Y|H^{(P)})}{f(Y|H^{(P)})}} \quad (4.9)$$

$$\text{where } f_i(Y|H^{(P)}) = \frac{1}{\sqrt{2\pi}\sigma} \exp\left\{-\frac{1}{2\sigma^2}\|Y - H^{(P)}X_i\|^2\right\}$$

$$f(Y|H^{(P)}) = \sum_{i=1}^M P(X_i) \cdot f_i(Y|H^{(P)})$$

$$P(X_i) = \prod_{j=1}^J \frac{\exp\{D(i, j)\lambda_2^{\pi\mathbf{P}}[d(n, j)]\}}{1 + \exp\{D(i, j)\lambda_2^{\pi\mathbf{P}}[d(n, j)]\}} \quad (4.10)$$

Eq.(4.10) is obtained by the following two definitions:

$$P(X_i) \triangleq P[X(n) = X_i] = \prod_{j=1}^J P[d(n, j) = D(i, j)]$$

$$\lambda_2^{\pi\mathbf{P}} \triangleq \log \frac{P[d(n, j) = +1]}{P[d(n, j) = -1]}.$$

3. Carrier Frequency Offset Estimation

In this section, we will study a FFT-based frequency offset estimation algorithm proposed in [5]. Consider the time domain model for an OFDM system with carrier frequency offset, and suppose P out of total N OFDM sub-carriers are used to transmit symbols:

$$\underline{r}(k) = \underbrace{F(\epsilon)W_P}_{\triangleq W_F} \underbrace{H\underline{S}(k)e^{j(k-1)(N+N_g)\frac{2\pi\epsilon}{N}}}_{\triangleq \underline{\alpha}(k)} + \underline{z}(k) \quad (4.11)$$

$$\text{with } \underline{S}(k) \triangleq [x(1), x(2), \dots, x(P)]^T_{\text{(the } k\text{th OFDM block)}}$$

$$\underline{r}(k) \triangleq [y(1), y(2), \dots, y(N)]^T_{\text{(the } k\text{th OFDM block)}}$$

$$F(\epsilon) \triangleq \text{diag}\{1, e^{j\frac{2\pi\epsilon}{N}}, \dots, e^{j\frac{2\pi\epsilon(N-1)}{N}}\}$$

$$H \triangleq \text{diag}\{H(1), H(2), \dots, H(P)\}$$

$$H(i) = \sum_{l=0}^{L-1} h(l) e^{-\frac{j2\pi l}{N} i}$$

$$W_P \triangleq \begin{pmatrix} 1 & 1 & \cdots & 1 \\ 1 & e^{j\frac{2\pi}{N}} & \cdots & e^{j(P-1)\frac{2\pi}{N}} \\ \vdots & \vdots & \ddots & \vdots \\ 1 & e^{j\frac{2\pi}{N}(N-1)} & \cdots & e^{j(P-1)\frac{2\pi}{N}(N-1)} \end{pmatrix}$$

In Eq. (4.11), assuming H and W_F are unknown but deterministic, then given the transmitted signal vector $\underline{S}(k)$, we can write the conditional probability density function of the received data vector $\underline{r}(k)$ as follows,

$$f(\underline{r}(k)|\underline{S}(k)) = \frac{1}{(\pi\sigma^2)^N} \exp\left\{-\frac{\|\underline{r}(k) - W_F \underline{\alpha}(k)\|^2}{\sigma^2}\right\}$$

The problem is to find the conditional maximum likelihood estimates of the carrier frequency offset ϵ and transmitted signal vector $\underline{S}(k)$, i.e.

$$\arg \max_{\epsilon, \underline{\alpha}(k)} f(\underline{r}(k)|\underline{S}(k)) \iff \arg \min_{\epsilon, \underline{\alpha}(k)} \|\underline{r}(k) - W_F \underline{\alpha}(k)\|^2$$

Recall in Eq. (4.11),

$$W_F \triangleq F(\epsilon) W_P = [F(\epsilon) \underline{w}_1, F(\epsilon) \underline{w}_2, \cdots, F(\epsilon) \underline{w}_P]$$

$$\text{define } \underline{e}_i = F(\epsilon) \underline{w}_i = [1, e^{j2\pi \frac{i-1+\epsilon}{N}}, \cdots, e^{j2\pi \frac{i-1+\epsilon}{N}(N-1)}]^T$$

$$\implies W_F = [\underline{e}_1, \underline{e}_2, \cdots, \underline{e}_P]$$

$$W_F^H W_F = N I_{P \times P}$$

First to find the estimate of ϵ ,

$$\hat{\epsilon} = \arg \max_{\epsilon} \left\{ \left\| W_F W_F^H \underline{r}(k) \right\|^2 \right\} \quad (4.12)$$

$$\begin{aligned}
& \left\| W_F W_F^H \underline{r}(k) \right\|^2 = \underline{r}(k)^H W_F W_F^H W_F W_F^H \underline{r}(k) \\
& = N \underline{r}(k)^H W_F W_F^H \underline{r}(k) \\
& = N \underline{r}(k)^H \sum_{i=1}^P \underline{e}_i \underline{e}_i^H \underline{r}(k) \\
& = N \sum_{i=1}^P \left| \underline{e}_i^H \underline{r}(k) \right|^2 \\
& = N \sum_{i=1}^P \left| \sum_{n=0}^{N-1} r(n) \exp\left\{ -j2\pi \frac{i-1+\epsilon}{N} n \right\} \right|^2 \\
& = N \sum_{i=1}^P \left| \sum_{n=0}^{N-1} \underbrace{\left(r(n) \exp\left\{ -j2\pi \frac{i-1}{N} n \right\} \right)}_{\triangleq r_i(n)} \exp\left\{ -j2\pi n \frac{\epsilon}{N} \right\} \right|^2 \\
& = N \sum_{i=1}^P \left| \sum_{n=0}^{N-1} r_i(n) \exp\left\{ -j2\pi n \frac{\epsilon}{N} \right\} \right|^2
\end{aligned}$$

Therefore, the maximization problem reduces to

$$\hat{\epsilon} = \arg \max_{\epsilon} \sum_{i=1}^P P_{r_i}(f_{\epsilon}),$$

where $P_{r_i}(f_{\epsilon}) \triangleq \frac{1}{N} \left| \sum_{n=0}^{N-1} r_i(n) e^{-j2\pi f_{\epsilon} n} \right|^2$, $f_{\epsilon} = \frac{\epsilon}{N}$

which can be computed by FFT algorithm. We can effectively increase the length of the sequence by means of zero-padding to achieve better frequency resolution.

C. Simulation Results

In this section, we present some simulation examples to illustrate the performance of the proposed iterative receiver in coded OFDM system with frequency offset and frequency selective fading. In the following simulations, QPSK constellation is used at the modulator. A rate 1/2 constraint length $\nu = 5$ convolutional code (with

generators [23, 35] in octal notation) is employed as the channel code. Simulations are carried out through an equal-power 4-tap frequency selective fading channel with 50Hz and 200Hz Doppler frequencies. The available bandwidth is 800kHz and is divided into 128 sub-carriers. The last eight sub-carriers are used as guard tones and the rest (120 tones) are used to transmit data. This corresponds to an OFDM word duration of 160 μ s. In each OFDM word, an additional guard interval of 40 μ s is added to combat with ISI due to the multi-path delay spread, hence the system has a total block length $T_f = 200\mu$ s and a sub-carrier symbol rate $R_b = 5$ kHz. In the following figures, 10–14, the performance is demonstrated in terms of bit-error-rate (BER) versus signal to noise ratio (SNR).

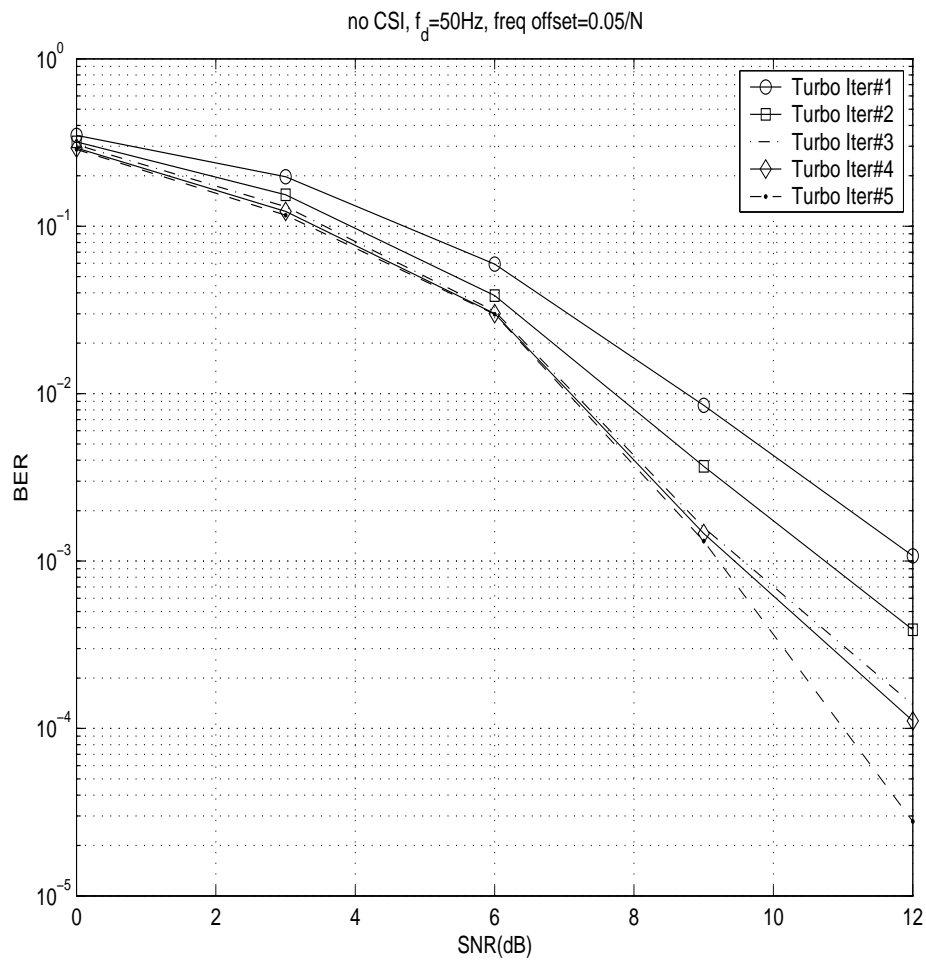


Fig. 10. BER in a coded OFDM system through a 4-tap frequency selective fading channel with Doppler shift $f_d = 50\text{Hz}$. Carrier frequency offset $f_\epsilon = 0.05/N$.

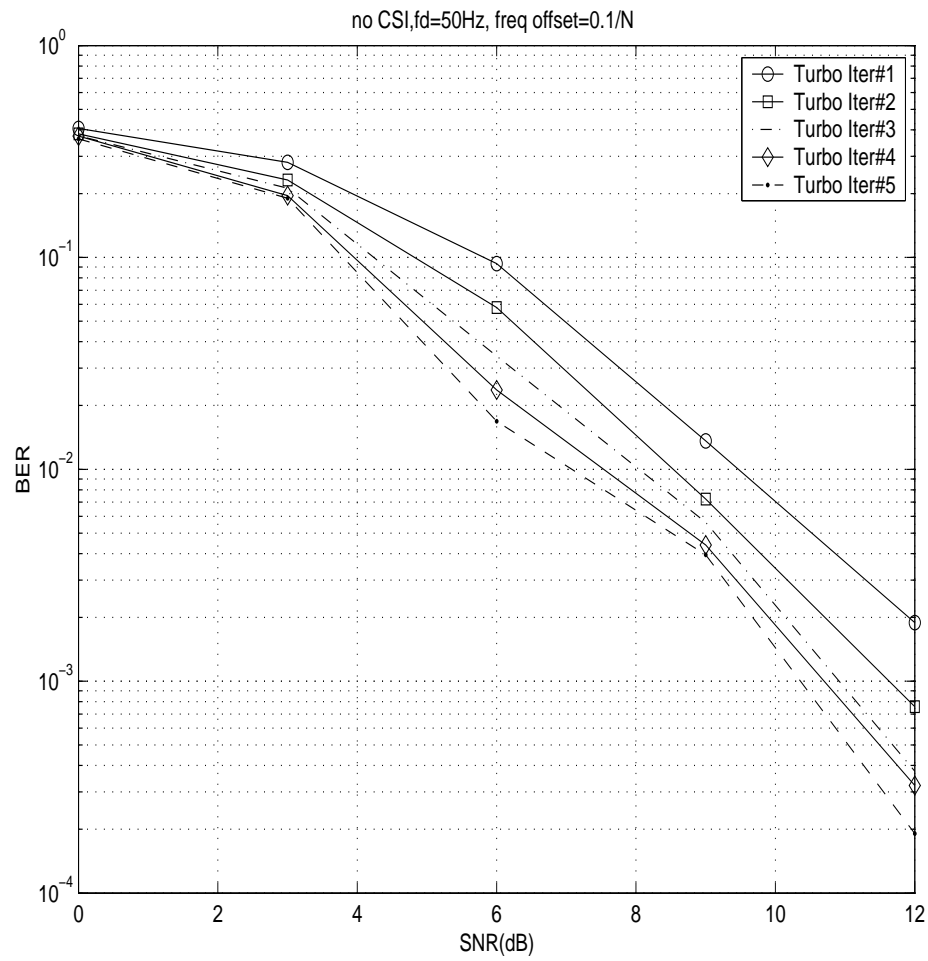


Fig. 11. BER in a coded OFDM system through a 4-tap frequency selective fading channel with Doppler shift $f_d = 50\text{Hz}$. Carrier frequency offset $f_\epsilon = 0.1/N$.

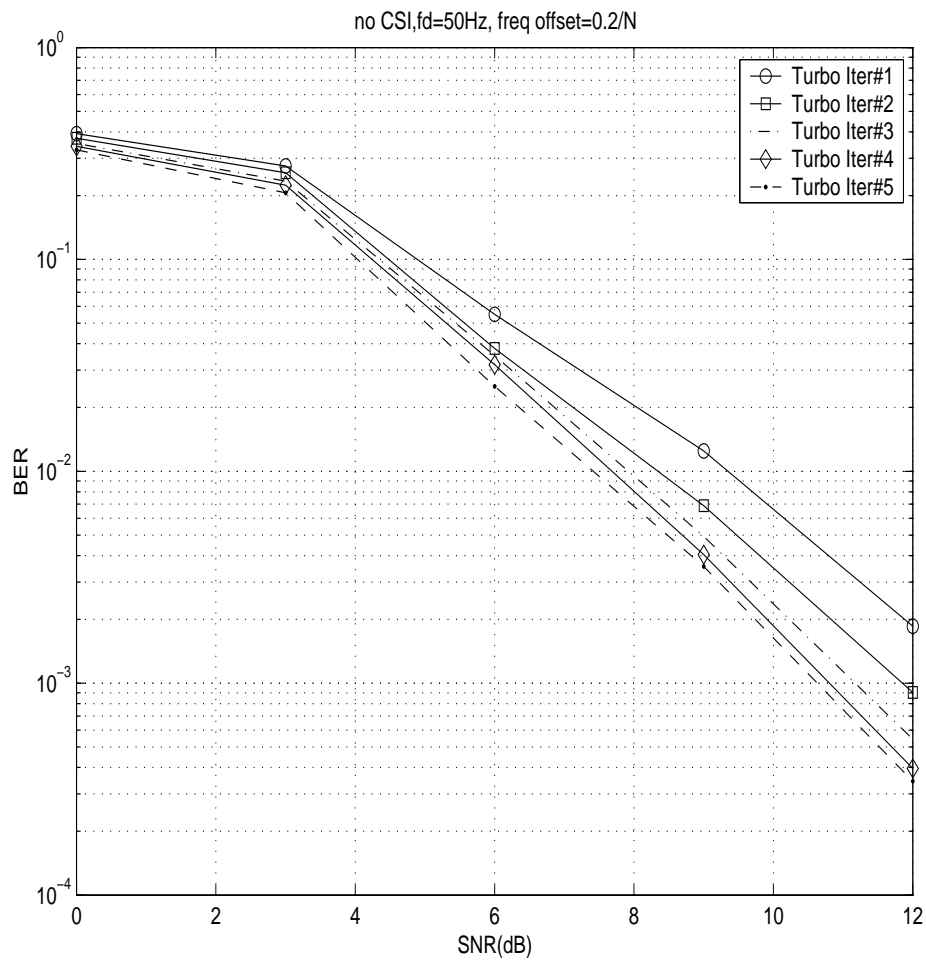


Fig. 12. BER in a coded OFDM system through a 4-tap frequency selective fading channel with Doppler shift $f_d = 50\text{Hz}$. Carrier frequency offset $f_\epsilon = 0.2/N$.

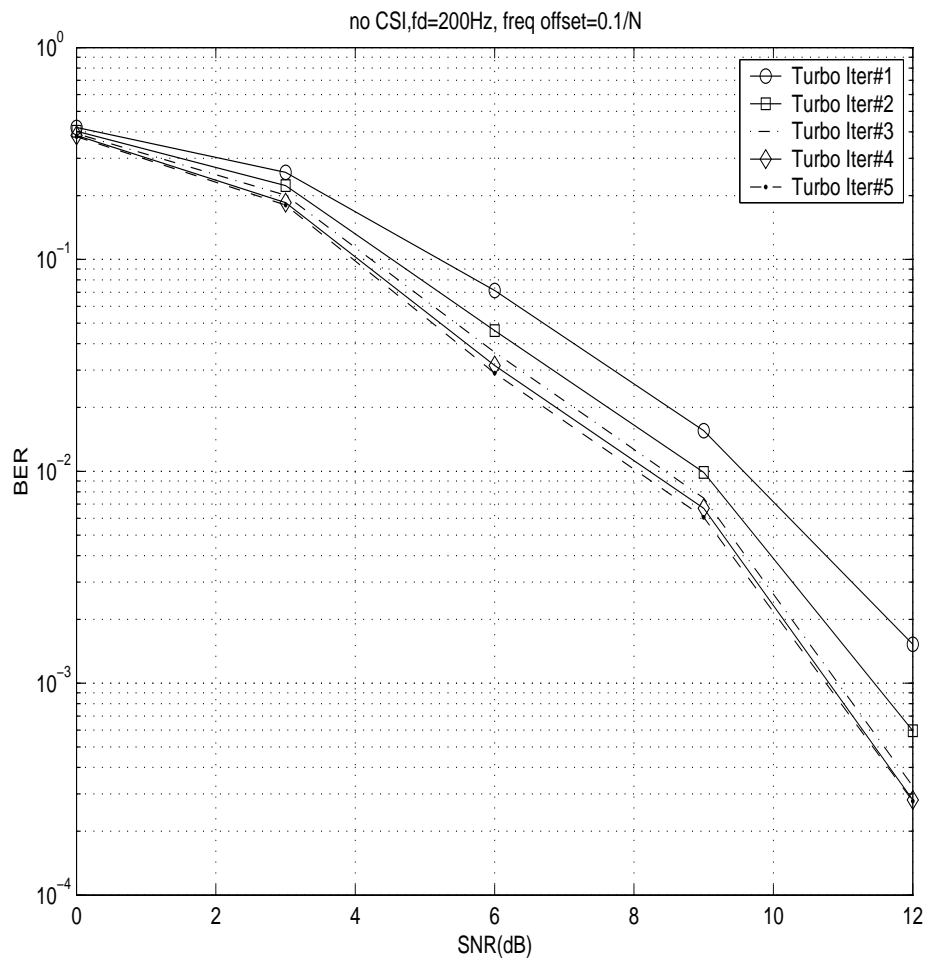


Fig. 13. BER in a coded OFDM system through a 4-tap frequency selective fading channel with Doppler shift $f_d = 200\text{Hz}$. Carrier frequency offset $f_\epsilon = 0.1/N$.

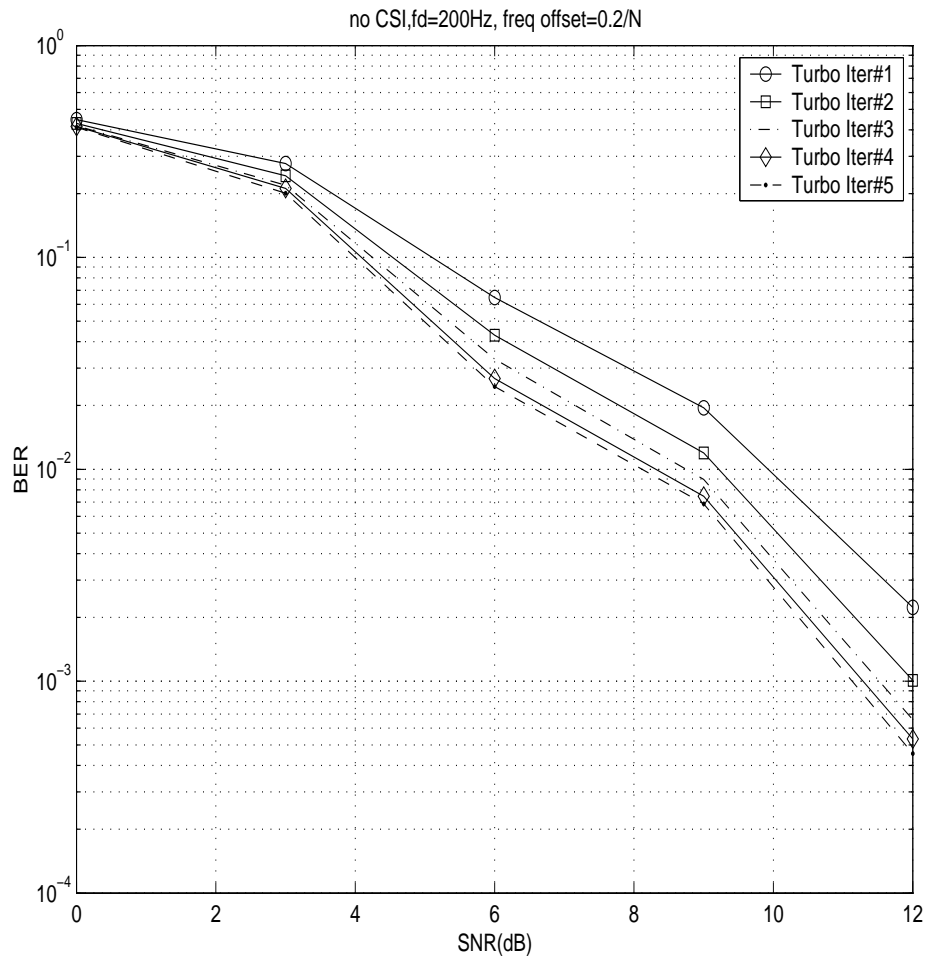


Fig. 14. BER in a coded OFDM system through a 4-tap frequency selective fading channel with Doppler shift $f_d = 200\text{Hz}$. Carrier frequency offset $f_\epsilon = 0.2/N$.

CHAPTER V

ITERATIVE RECEIVER FOR STBC-OFDM SYSTEM

Space-time coding (STC) methodologies [11], including space-time trellis coding (STTC) and space-time block coding (STBC), integrate the techniques of antenna array spatial diversity and channel coding, and can provide significant capacity gains in wireless channels. Since space-time codes are originally designed for flat-fading channels, it is challenging to apply them over multi-path fading channels. One approach is to employ OFDM which convert a multi-path channel into parallel independent frequency-flat sub-channels.

In STBC-OFDM, channel state information between each transmit and receive antenna pair is required for coherent decoding. However, for each OFDM tone, since the received signals are a superposition of signals transmitted from different antennas, the simple techniques used in single antenna cases cannot be easily applied. Here for STBC-OFDM system employing outer channel codes, we will introduce an iterative receiver, by applying the algorithm of channel estimation described in [11] with simplifications. The proposed turbo receiver will iterate between the maximum *a posteriori* (MAP)-EM STBC decoding stage and the SISO channel decoding stage, to successively improve the system performance.

Furthermore, STBC-OFDM systems still suffer from severe performance degradation due to carrier frequency offset. Over the past years, extensive research work has been undertaken to design both data-aided and blind frequency synchronization algorithms for OFDM systems. However, most existing frequency estimation techniques rely on periodic transmission of reference symbols, hence reducing the bandwidth efficiency. Some of them suggest training symbol structure specialized for synchronization but do not take into account the channel estimation that also needs to be

done, while others have certain limit working range due to the mod 2π ambiguity and cannot be applied to large frequency offset cases. Moreover, very few of them are applied to STBC-OFDM systems. In my work, I will extend the algorithm [5] for frequency offset correction designed for single antenna OFDM systems to STBC-OFDM systems. This algorithm combines the conditional maximum likelihood approach and the low-rank property of the narrow-band sub-channels. It also takes advantage of available multiple frames of received data to refine the carriers offset estimation.

This chapter is outlined as follows. In section A, the STBC-OFDM system model will be given. In section B, we will introduce the iterative receiver for STBC-OFDM system in the presence of carrier frequency offset and dispersive fading.

A. The System Model

1. STBC Encoding Algorithm

A general STBC is defined by a $(P \times K)$ code matrix \mathcal{G} , where K denotes the number of transmitter antennas, and P is the number of time slots for transmitting an STBC codeword. Each row of \mathcal{G} is a permuted and transformed (i.e., negated and/or conjugated) form of the K dimensional vector of complex data symbols \underline{x} . As a simple example, we consider a 2×2 (i.e., $P = 2$, $K = 2$) STBC with code matrix

$$\mathcal{G}_1 = \begin{bmatrix} x_1 & x_2 \\ -x_2^* & x_1^* \end{bmatrix}$$

The input to this STBC is data vector $\underline{x} = [x_1, x_2]^T$. During the first time slot, the two symbols in the first row of \mathcal{G} , i.e., $[x_1, x_2]$, are transmitted from the two transmitter antennas simultaneously; similarly in the second time slot, the symbols in the second row, $[-x_2^*, x_1^*]$, are transmitted.

In an STBC-OFDM system, we use the above STBC to independently encode the data symbols transmitted at different OFDM sub-carriers. For instance, at the k -th OFDM sub-carrier, during the first time slot, two data symbols $[x_1[1, k], x_2[1, k]]$ are transmitted simultaneously from the two antennas; while during the second time slot, symbols in $[-x_2^*[1, k], x_1^*[1, k]]$ are transmitted.

2. STBC-OFDM System Model

We consider a STBC-OFDM system with N sub-carriers, 2 transmitter antennas and 1 receiver, signaling through a frequency and time selective fading channel. Under the assumption that the fading channel coefficients remain constant through the interval of a STBC word, namely two consecutive OFDM words, the system model is given by:

$$\underline{Y} = XW\underline{h} + \underline{Z} = X\underline{H} + \underline{Z} \quad (5.1)$$

where

$$\underline{Y} \triangleq \begin{bmatrix} \underline{y}(1)^T, \underline{y}(2)^T \end{bmatrix}_{(2N) \times 1}^T,$$

$$\underline{y}(p) \triangleq [y(p, 1), y(p, 2), \dots, y(p, N)]_{N \times 1}^T, \quad p = 1, 2,$$

$$X \triangleq \begin{pmatrix} X_1(1) & X_2(1) \\ X_1(2) & X_2(2) \end{pmatrix} = \begin{pmatrix} X_1(1) & X_2(1) \\ -X_2(1)^* & X_1(1)^* \end{pmatrix}_{(2N) \times (2N)}$$

$$X_i(p) \triangleq \begin{pmatrix} x_i(p, 1) & 0 & \dots & 0 \\ 0 & x_i(p, 2) & \dots & 0 \\ \vdots & \vdots & \ddots & \vdots \\ 0 & 0 & \dots & x_i(p, N) \end{pmatrix}$$

$$\underline{h} \triangleq [\underline{h}_1^T, \underline{h}_2^T]_{(2L) \times 1}^T$$

$$\underline{h}_i \triangleq [h_i(1), h_i(2), \dots, h_i(L)]^T$$

$$\begin{aligned} \underline{H} &\triangleq [\underline{H}_1^T, \underline{H}_2^T]_{(2N) \times 1}^T \\ \underline{H}_i &\triangleq \text{DFT}_N(\underline{h}_i) = [H_i(1), H_i(2), \dots, H_i(N)]^T \\ W &\triangleq \begin{pmatrix} \omega_{L(N \times L)} & 0 & (N \times L) \\ 0 & (N \times L) & \omega_{L(N \times L)} \end{pmatrix} \\ \text{with } \omega_L &\triangleq \begin{pmatrix} 1 & 1 & \dots & 1 \\ 1 & e^{-j\frac{2\pi}{N}} & \dots & e^{-j(L-1)\frac{2\pi}{N}} \\ \vdots & \vdots & \ddots & \vdots \\ 1 & e^{-j\frac{2\pi}{N}(N-1)} & \dots & e^{-j(L-1)\frac{2\pi}{N}(N-1)} \end{pmatrix} \end{aligned}$$

$X_i(p)$ represents the transmitted data sequence from the i -th antenna at the p -th time slot, and $\underline{y}(p)$ represents the received data sequence at the p -th time slot. h_i is the L -sized vector containing the time domain responses of all the taps from the i -th transmitter. Because of the constant norm of the transmitted M -PSK symbols and the orthogonality property of STBC codes, we have:

$$W^H X^H X W = (PN) \cdot I_{(PN) \times (PN)}, \quad P = 2. \quad (5.2)$$

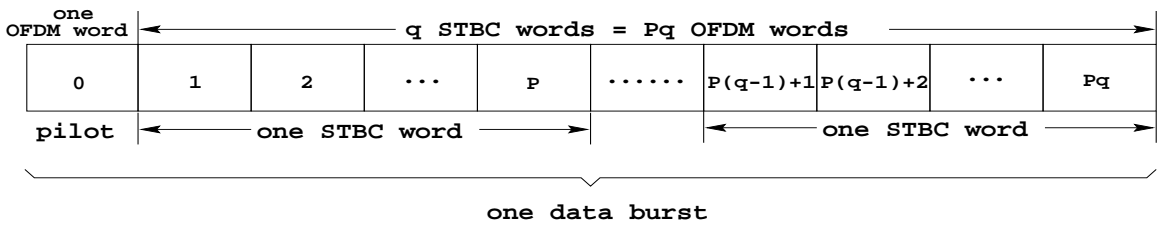


Fig. 15. A data burst.

As in a typical data communication scenario, communication is carried out in a burst manner. A data burst (Fig.15) spans $(Pq + 1)$ OFDM words, with the first OFDM word containing the optimal training symbols. The rest (Pq) OFDM words

contain q STBC code words.

B. Receiver Structure

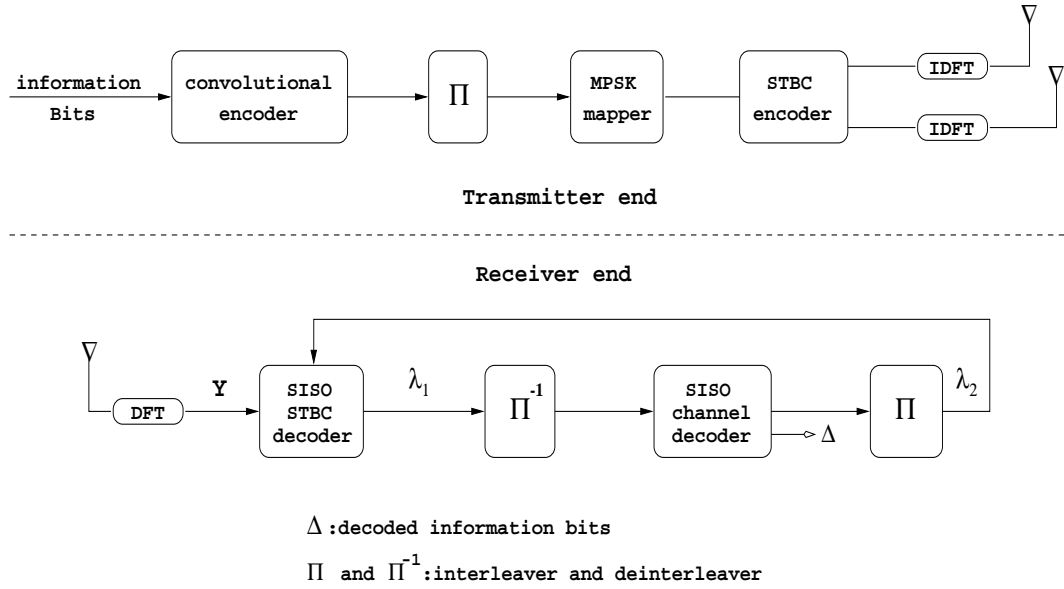


Fig. 16. A coded STBC-OFDM system with iterative receiver.

As depicted in Fig.16, the information bits are first encoded by a convolutional encoder and interleaved. Then the interleaved code bits are modulated by an MPSK modulator. Finally the modulated MPSK symbols are encoded by a STBC encoder and transmitted from 2 transmitter antennas across 2 consecutive OFDM slots at a particular OFDM sub-carrier. During 2 OFDM slots, altogether N STBC code words are transmitted. The receiver end contains of an SISO STBC decoder and an SISO channel decoder. During each turbo iteration, the extrinsic *a priori* LLR's $\{\lambda_2\}$ from the previous iteration are provided by the channel decoder, and sent back to the STBC decoder, which in turn computes the extrinsic *a posteriori* LLR's $\{\lambda_1\}$ and feeds them back to the channel decoder to complete one iteration. At the last

iteration, hard decisions of the information bits are given by the channel decoder.

1. SISO STBC Decoder

Consider the problem of estimating transmitted data X in Eq.(5.1). The MAP estimate \hat{X} of X is a solution to

$$\hat{X} = \arg \max_X \log p(X|\underline{Y}) \Leftrightarrow \arg \max_X \left(\log p(\underline{Y}|X) + \log p(X) \right). \quad (5.3)$$

The MAP-EM algorithm [11] solves problem (5.3) iteratively according to the following two steps:

- E – step : $Q(X|X^{(P)}) = E_{\underline{h}|\underline{Y}, X^{(P)}} \left\{ \log f(\underline{Y}|X, \underline{h}) | \underline{Y}, X^{(P)} \right\}$
- M – step : $X^{(P+1)} = \arg \max_X [Q(X|X^{(P)}) + \log p(X)]$.

Suppose $\underline{h} \sim \mathcal{N}(\underline{0}, \Sigma_{\underline{h}})$, $\underline{Z} \sim \mathcal{N}(\underline{0}, \Sigma)$, where $\Sigma_{\underline{h}} \triangleq E\{\underline{h} \underline{h}^H\}$ and $\Sigma \triangleq E\{\underline{Z} \underline{Z}^H\}$, and define $\Theta = X^{(P)}W$. Notice that given $X^{(P)}$, \underline{Y} and \underline{h} are jointly Gaussian with mean vector $\underline{\mu}_{\underline{Y}}$ and $\underline{\mu}_{\underline{h}}$, covariance matrices $\Sigma_{\underline{Y}}$ and $\Sigma_{\underline{h}}$, and cross-covariance matrix $\Sigma_{\underline{h}\underline{Y}} \triangleq E\{(\underline{h} - \underline{\mu}_{\underline{h}})(\underline{Y} - \underline{\mu}_{\underline{Y}})^H\}$, i.e.,

$$\begin{bmatrix} \underline{Y} \\ \underline{h} \end{bmatrix} \sim \mathcal{N} \left(\begin{bmatrix} \underline{\mu}_{\underline{Y}} \\ \underline{\mu}_{\underline{h}} \end{bmatrix}, \begin{bmatrix} \Sigma_{\underline{Y}} & \Sigma_{\underline{h}\underline{Y}}^H \\ \Sigma_{\underline{h}\underline{Y}} & \Sigma_{\underline{h}} \end{bmatrix} \right),$$

with $\underline{\mu}_{\underline{Y}} = \Theta \underline{\mu}_{\underline{h}} = \underline{0}$, $\Sigma_{\underline{Y}} = \Theta \Sigma_{\underline{h}} \Theta^H + \Sigma$, and $\Sigma_{\underline{h}\underline{Y}} = \Sigma_{\underline{h}} \Theta^H$.

Within this model, it is straightforward to show that the conditional distribution of the random parameter vector \underline{h} given the observed data \underline{Y} and assuming that $X = X^{(P)}$ is also Gaussian, i.e., $\underline{h}|\underline{Y}, X^{(P)} \sim \mathcal{N}(\hat{\underline{h}}, \hat{\Sigma}_{\underline{h}})$. According to [9], we have

$$\begin{aligned} \hat{\underline{h}} &= \underline{\mu}_{\underline{h}} + \Sigma_{\underline{h}} \Theta^H (\Theta \Sigma_{\underline{h}} \Theta^H + \Sigma)^{-1} (\underline{Y} - \Theta \underline{\mu}_{\underline{h}}) \\ &= \underline{\mu}_{\underline{h}} + (\Theta^H \Sigma^{-1} \Theta + \Sigma_{\underline{h}}^{-1})^{-1} \Theta^H \Sigma^{-1} (\underline{Y} - \Theta \underline{\mu}_{\underline{h}}) \end{aligned}$$

$$\begin{aligned}
&= (\Theta^H \Sigma^{-1} \Theta + \Sigma_{\underline{h}}^{-1})^{-1} \Theta^H \Sigma^{-1} \underline{Y} \\
\hat{\Sigma}_{\underline{h}} &= \Sigma_{\underline{h}} - \Sigma_{\underline{h}} \Theta^H (\Theta \Sigma_{\underline{h}} \Theta^H + \Sigma)^{-1} \Theta \Sigma_{\underline{h}} \\
&= \Sigma_{\underline{h}} - (\Theta^H \Sigma^{-1} \Theta + \Sigma_{\underline{h}}^{-1})^{-1} \Theta^H \Sigma^{-1} \Theta \Sigma_{\underline{h}}
\end{aligned}$$

If we further assume that channels of different paths or between different transmitter-receiver pairs are uncorrelated, all channels are of equal power, and noise process is white, then we can get $\Sigma_{\underline{h}} = \frac{1}{L} \mathbf{I}_{(2L) \times (2L)}$, $\Sigma = \sigma^2 \mathbf{I}_{(2N) \times (2N)}$. Then using property (5.2), $\hat{\underline{h}}$ and $\hat{\Sigma}_{\underline{h}}$ can be simplified to:

$$\hat{\underline{h}} = \frac{1}{PN + \sigma^2 L} \Theta^H \underline{Y} \quad (5.4)$$

$$\hat{\Sigma}_{\underline{h}} = \frac{\sigma^2}{PN + \sigma^2 L} \mathbf{I}_{(2L) \times (2L)}. \quad (5.5)$$

Considering (5.2), (5.4) and (5.5), and the property that $\text{trace}(\mathbf{AB}) = \text{trace}(\mathbf{BA})$, $Q(X|X^{(P)})$ given in [6] can be simplified to:

$$\begin{aligned}
Q(X|X^{(P)}) &= -\frac{1}{\sigma^2} \left[\|\underline{Y} - XW\hat{\underline{h}}\|^2 + \text{trace}\{XW\hat{\Sigma}_{\underline{h}}W^H X^H\} \right] + \text{const.} \\
&= -\frac{1}{\sigma^2} \|\underline{Y} - XW\hat{\underline{h}}\|^2 + \text{const.} \\
&= \sum_{n=0}^{N-1} \sum_{p=1}^P -\frac{1}{\sigma^2} \underbrace{\left| y(p, n) - x_1(p, n)\hat{H}_1(n) - x_2(p, n)\hat{H}_2(n) \right|^2}_{\triangleq q[\underline{x}(p, n)]} + \text{const.},
\end{aligned}$$

where $\underline{x}(p, n) \triangleq [x_1(p, n), x_2(p, n)]^T$. Then in the M-step,

$$\begin{aligned}
X^{(P+1)} &= \arg \max_X [Q(X|X^{(P)}) + \log p(X)] \\
&= \sum_{n=0}^{N-1} \arg \min_{\underline{x}(1, n)} \left[\frac{1}{\sigma^2} \sum_{p=1}^P q[\underline{x}(p, n)] - \log p[\underline{x}(1, n)] \right]. \quad (5.6)
\end{aligned}$$

Note that the maximization problem decoupled into N independent minimization problems under the assumption that the outer channel code bits are ideally interleaved and thus $\underline{x}(p, n)$ at different OFDM sub-carriers are independent.

Recall in one STBC-OFDM word duration, at the n -th OFDM sub-carrier, K transmitters transmit K MPSK symbols, which correspond to $J = K \log_2 |\Omega_c|$ outer channel code bits $\{d(n, 1), d(n, 2), \dots, d(n, J)\}$, where Ω_c is the set of M -PSK symbols. Then the extrinsic *a posteriori* LLR of $d(n, j)$ at the output of the STBC decoder can be computed as follows:

$$\begin{aligned}
\lambda_1^\pi[d(n, j)] &\triangleq \Lambda_1^\pi[d(n, j)] - \lambda_2^{\pi\mathbf{P}}[d(n, j)] \quad j = 1, 2, \dots, J \\
&= \log \frac{P[d(n, j) = +1|\mathbf{Y}]}{P[d(n, j) = -1|\mathbf{Y}]} - \log \frac{P[d(n, j) = +1]}{P[d(n, j) = -1]} \\
&= \log \frac{\sum_{\underline{x}(1) \in \underline{x}_j^+} p[\underline{x}(1, n) = \underline{x}(1)|\mathbf{Y}]}{\sum_{\underline{x}(1) \in \underline{x}_j^-} p[\underline{x}(1, n) = \underline{x}(1)|\mathbf{Y}]} - \lambda_2^{\pi\mathbf{P}}[d(n, j)] \\
&= \log \frac{\sum_{\underline{x}(1) \in \underline{x}_j^+} \exp\left\{-\frac{1}{\sigma^2} \sum_{p=1}^P q[\underline{x}(p, n)|\underline{x}(1, n) = \underline{x}(1)]\right\} \cdot p[\underline{x}(1, n) = \underline{x}(1)]}{\sum_{\underline{x}(1) \in \underline{x}_j^-} \exp\left\{-\frac{1}{\sigma^2} \sum_{p=1}^P q[\underline{x}(p, n)|\underline{x}(1, n) = \underline{x}(1)]\right\} \cdot p[\underline{x}(1, n) = \underline{x}(1)]} \\
&\quad - \lambda_2^{\pi\mathbf{P}}[d(n, j)],
\end{aligned}$$

$$\begin{aligned}
\text{with } p[\underline{x}(1, n) = \underline{x}(1)] &= \prod_{j=1}^J p[d(n, j) = D(j)] \\
&= \prod_{j=1}^J \frac{\exp\{D(j)\lambda_2^{\pi\mathbf{P}}[d(n, j)]\}}{1 + \exp\{D(j)\lambda_2^{\pi\mathbf{P}}[d(n, j)]\}}, \quad D(i) \in \{+1, -1\}.
\end{aligned}$$

\underline{x}_j^+ and \underline{x}_j^- , each represents the set of $\underline{x}(1)$'s, of which the j -th outer channel code bit is +1, -1, respectively.

Next we briefly show the initialization of the discussed MAP-EM algorithm. First, channel estimation is done by exploiting the time domain correlation of the fading channel, which has been given in chapter 3. Secondly, based on the channel estimate, $\underline{X}^{(0)}$ is obtained by the traditional ML algorithm.

Denote $\{h_i(l, 1), h_i(l, 2), \dots, h_i(l, k-1), h_i(l, k), h_i(l, k+1), \dots\}$ the fading process of the l -th path, of the channel between the i -th transmitter and the receiver, where

k is the time index, representing the k -th OFDM block. We want to estimate $h_i(l, k)$ using the channel estimates of the past (LL) OFDM blocks, i.e.,

$$\tilde{h}_i(l, k) = \sum_{j=1}^{LL} \alpha_j h_i(l, k - j), \quad l = 1, 2, \dots, L, \quad (5.7)$$

where $\{\alpha_j\}_{j=1}^{LL}$ is such that:

$$\mathbb{E}\left\{[\tilde{h}_i(l, k) - h_i(l, k)] h_i^*(l, k - j)\right\} = 0, \quad j = 1, 2, \dots, LL. \quad (5.8)$$

After some manipulations, we have as follows:

$$\underbrace{\begin{pmatrix} R[0] & R[-1] & \cdots & R[-LL-1] \\ R[1] & R[0] & \cdots & R[-LL-2] \\ \vdots & \vdots & \ddots & \vdots \\ R[LL-1] & R[LL-2] & \cdots & R[0] \end{pmatrix}}_{\bar{R}_t} \underbrace{\begin{pmatrix} \alpha_1 \\ \alpha_2 \\ \vdots \\ \alpha_{LL} \end{pmatrix}}_{\vec{\alpha}} = \underbrace{\begin{pmatrix} R[1] \\ R[2] \\ \vdots \\ R[LL] \end{pmatrix}}_{\vec{r}_t} \quad (5.9)$$

$$\implies \vec{\alpha} = \bar{R}_t^{-1} \cdot \vec{r}_t, \quad (5.10)$$

with $R[n] \triangleq R[nT_f] = J_0(2\pi f_d \cdot nT_f)$, where T_f is the OFDM block length and $J_0(\cdot)$ is the zeroth-order Bessel function of the first kind.

2. Carrier Frequency Offset Estimation

Consider the time domain model for an STBC-OFDM system with carrier frequency offset (two transmitters and one receiver), and suppose at each transmitter end, P out of total N OFDM sub-carriers are used to transmit symbols:

$$\underline{r}(k) = \underbrace{F(\epsilon)W_P}_{\triangleq W_F} \underbrace{\left(H_1 \underline{S}_1(k) + H_2 \underline{S}_2(k)\right)}_{\triangleq \underline{\alpha}(k)} e^{j(k-1)(N+N_g)\frac{2\pi\epsilon}{N}} + \underline{z}(k) \quad (5.11)$$

$$\begin{aligned}
\text{with } \underline{S}_n(k) &\triangleq [x_n(1), x_n(2), \dots, x_n(P)]_{(\text{the } k\text{th OFDM block})}^T \quad n = 1, 2 \\
\underline{r}(k) &\triangleq [y(1), y(2), \dots, y(N)]_{(\text{the } k\text{th OFDM block})}^T \\
F(\epsilon) &\triangleq \text{diag}\{1, e^{j\frac{2\pi\epsilon}{N}}, \dots, e^{j\frac{2\pi\epsilon(N-1)}{N}}\} \\
H_n &\triangleq \text{diag}\{H_n(1), H_n(2), \dots, H_n(P)\} \quad n = 1, 2 \\
H_n(i) &= \sum_{l=0}^{L-1} h_n(l) e^{-j\frac{2\pi l}{N}i} \\
W_P &\triangleq \begin{pmatrix} 1 & 1 & \dots & 1 \\ 1 & e^{j\frac{2\pi}{N}} & \dots & e^{j(P-1)\frac{2\pi}{N}} \\ \vdots & \vdots & \ddots & \vdots \\ 1 & e^{j\frac{2\pi}{N}(N-1)} & \dots & e^{j(P-1)\frac{2\pi}{N}(N-1)} \end{pmatrix}
\end{aligned}$$

In Eq. (5.11), assuming H_1, H_2 and W_F are unknown but deterministic, then given the transmitted signal vectors $\underline{S}_1(k)$ and $\underline{S}_2(k)$, we can write the conditional probability density function of the received data vector $\underline{r}(k)$ as follows,

$$f(\underline{r}(k)|\underline{s}_1(k), \underline{s}_2(k)) = \frac{1}{(\pi\sigma^2)^N} \exp\left\{-\frac{\|\underline{r}(k) - W_F \underline{\alpha}(k)\|^2}{\sigma^2}\right\}$$

The problem is to find the conditional maximum likelihood estimates of the carrier frequency offset ϵ and transmitted signal vectors $\underline{S}_1(k)$ and $\underline{S}_2(k)$, i.e.

$$\arg \max_{\epsilon, \underline{\alpha}(k)} f(\underline{r}(k)|\underline{S}_1(k), \underline{S}_2(k)) \iff \arg \min_{\epsilon, \underline{\alpha}(k)} \|\underline{r}(k) - W_F \underline{\alpha}(k)\|^2$$

Recall in Eq. (5.11),

$$\begin{aligned}
W_F &\triangleq F(\epsilon)W_P = [F(\epsilon)\underline{w}_1, F(\epsilon)\underline{w}_2, \dots, F(\epsilon)\underline{w}_P] \\
\text{define } \underline{e}_i &= F(\epsilon)\underline{w}_i = [1, e^{j2\pi\frac{i-1+\epsilon}{N}}, \dots, e^{j2\pi\frac{i-1+\epsilon}{N}(N-1)}]^T \\
\implies W_F &= [\underline{e}_1, \underline{e}_2, \dots, \underline{e}_P] \\
W_F^H W_F &= N I_{P \times P}
\end{aligned}$$

First to find the estimate of ϵ ,

$$\hat{\epsilon} = \arg \max_{\epsilon} \left\{ \left\| W_F W_F^H \underline{r}(k) \right\|^2 \right\} \quad (5.12)$$

$$\begin{aligned} \left\| W_F W_F^H \underline{r}(k) \right\|^2 &= \underline{r}(k)^H W_F W_F^H W_F W_F^H \underline{r}(k) \\ &= N \underline{r}(k)^H W_F W_F^H \underline{r}(k) \\ &= N \underline{r}(k)^H \sum_{i=1}^P \underline{e}_i \underline{e}_i^H \underline{r}(k) \\ &= N \sum_{i=1}^P \left| \underline{e}_i^H \underline{r}(k) \right|^2 \\ &= N \sum_{i=1}^P \left| \sum_{n=0}^{N-1} r(n) \exp\left\{ -j2\pi \frac{i-1+\epsilon}{N} n \right\} \right|^2 \\ &= N \sum_{i=1}^P \left| \sum_{n=0}^{N-1} \underbrace{\left(r(n) \exp\left\{ -j2\pi \frac{i-1}{N} n \right\} \right)}_{\triangleq r_i(n)} \exp\left\{ -j2\pi n \frac{\epsilon}{N} \right\} \right|^2 \\ &= N \sum_{i=1}^P \left| \sum_{n=0}^{N-1} r_i(n) \exp\left\{ -j2\pi n \frac{\epsilon}{N} \right\} \right|^2 \end{aligned}$$

Therefore, the maximization problem reduces to

$$\hat{\epsilon} = \arg \max_{\epsilon} \sum_{i=1}^P P_{r_i}(f_{\epsilon}),$$

where $P_{r_i}(f_{\epsilon}) \triangleq \frac{1}{N} \left| \sum_{n=0}^{N-1} r_i(n) e^{-j2\pi f_{\epsilon} n} \right|^2$, $f_{\epsilon} = \frac{\epsilon}{N}$

which can be computed by FFT algorithm. We can effectively increase the length of the sequence by means of zero-padding to achieve better frequency resolution.

C. Simulation Results

In this section, we present some simulation results to illustrate the performance of the proposed iterative receiver for STBC-OFDM system with outer channel code, in the presence of frequency offset and frequency selective fading. In the following simulations, QPSK constellation is used at the modulator. A rate $1/2$ constraint length $\nu = 5$ convolutional code (with generators [23, 35] in octal notation) is employed as the channel code. Simulations are carried out through an equal-power 4-tap frequency selective fading channel with 50Hz and 200Hz Doppler frequencies. The available bandwidth is 800kHz and is divided into 128 sub-carriers. The last eight sub-carriers are used as guard tones and the rest (120 tones) are used to transmit data. This corresponds to an OFDM word duration of $160\mu s$. In each OFDM word, an additional guard interval of $40\mu s$ is added to combat with ISI due to the multipath delay spread, hence the system has a total block length $T_f = 200\mu s$ and a sub-carrier symbol rate $R_b = 5\text{kHz}$. For all the simulations, two transmitter antennas and one receiver antenna are used; and the \mathcal{G}_1 STBC is adopted. The OFDM system transmits in a burst manner, i.e., each data burst includes 11 OFDM words, the first OFDM word contains optimal training symbols and the rest 10 OFDM words contain 5 STBC code words. In the following figures, 17–22, the performance is demonstrated in terms of bit-error-rate (BER) versus signal to noise ratio (SNR).

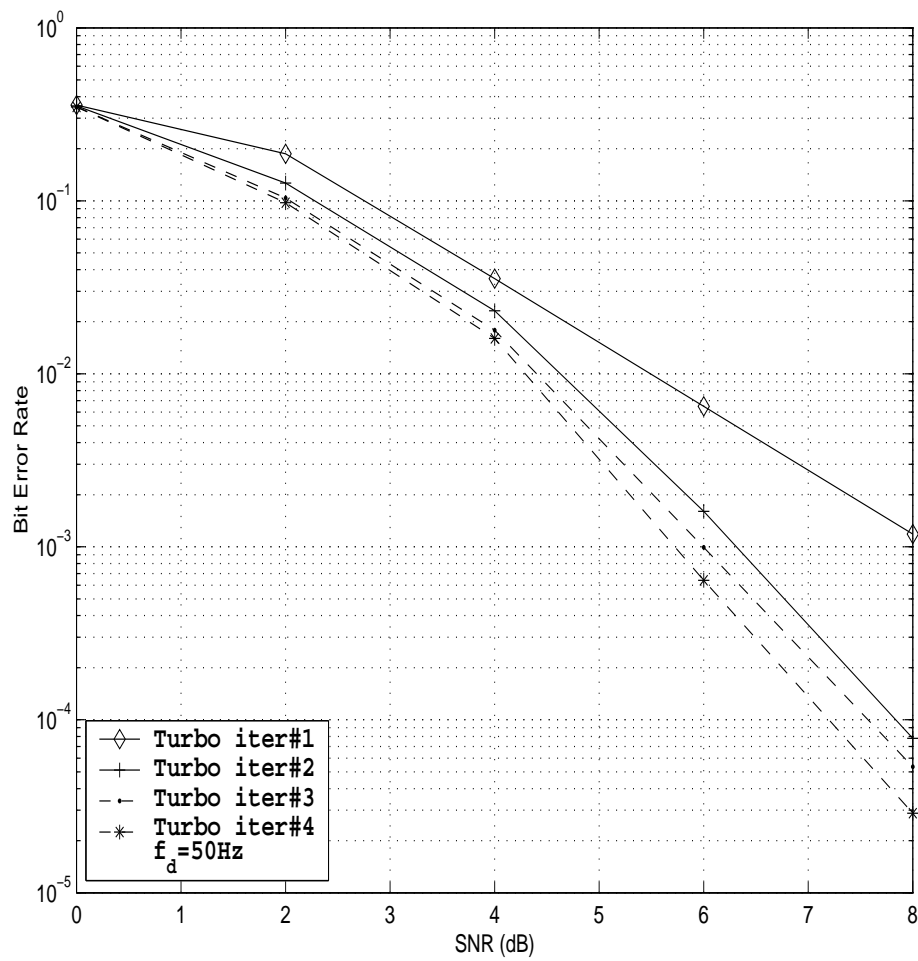


Fig. 17. BER in a coded STBC-OFDM system through a 4-tap frequency selective fading channel with Doppler shift $f_d = 50\text{Hz}$.

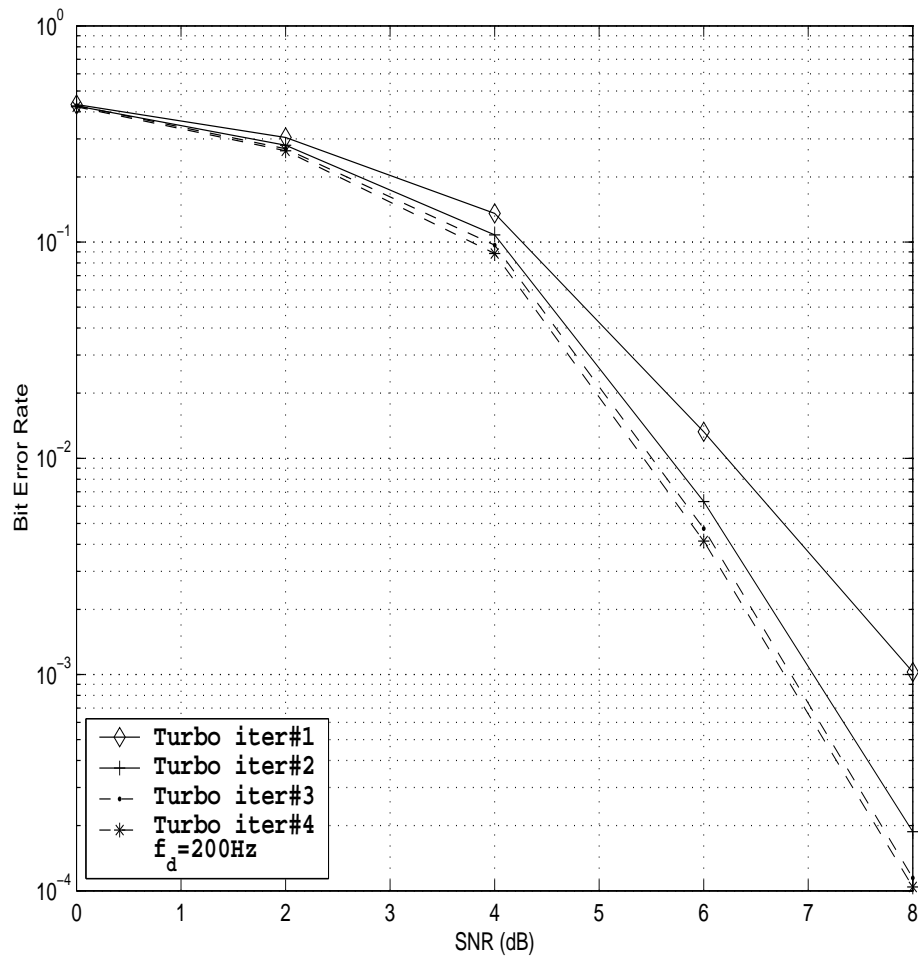


Fig. 18. BER in a coded STBC-OFDM system through a 4-tap frequency selective fading channel with Doppler shift $f_d = 200\text{Hz}$.

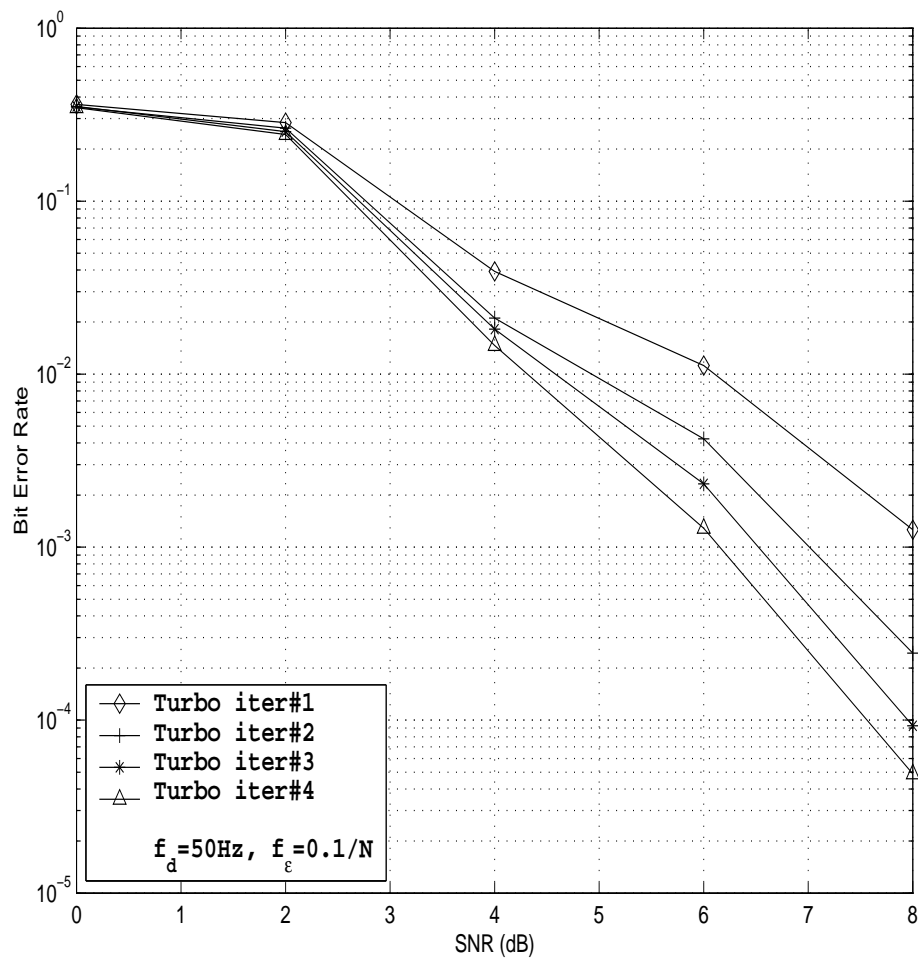


Fig. 19. BER in a coded STBC-OFDM system through a 4-tap frequency selective fading channel with Doppler shift $f_d = 50\text{Hz}$. Carrier frequency offset $f_\epsilon = 0.1/N$.

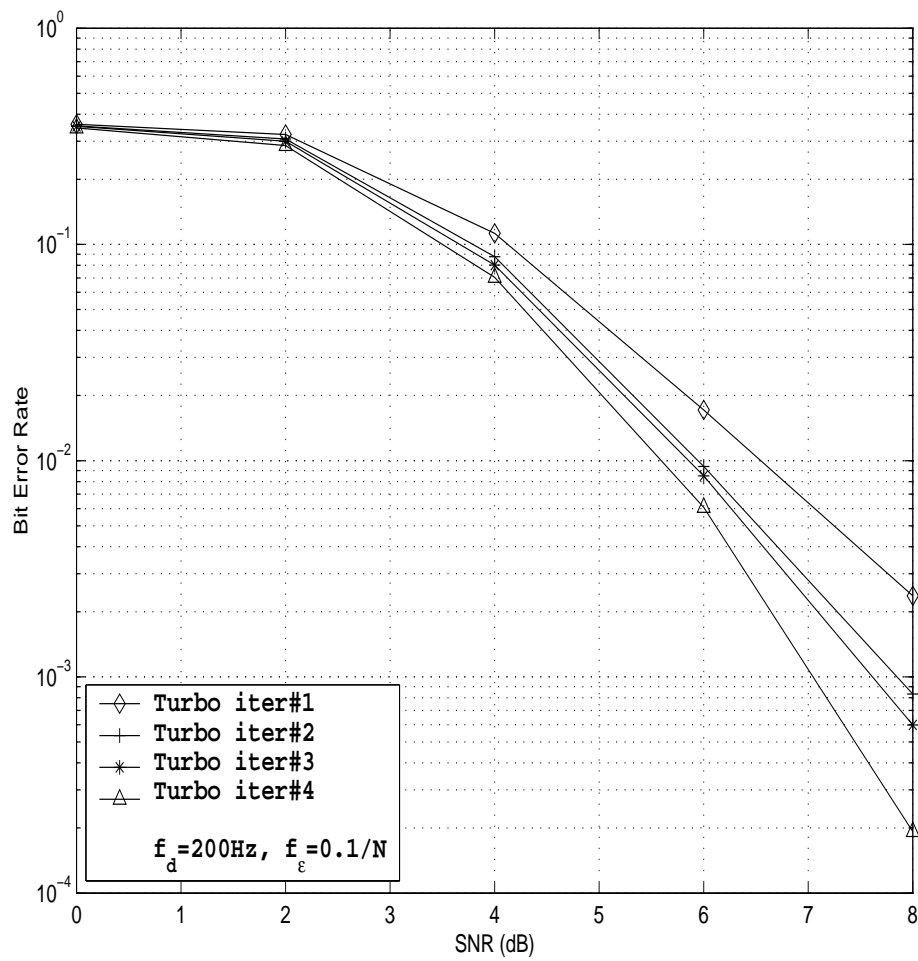


Fig. 20. BER in a coded STBC-OFDM system through a 4-tap frequency selective fading channel with Doppler shift $f_d = 200\text{Hz}$. Carrier frequency offset $f_\epsilon = 0.1/N$.

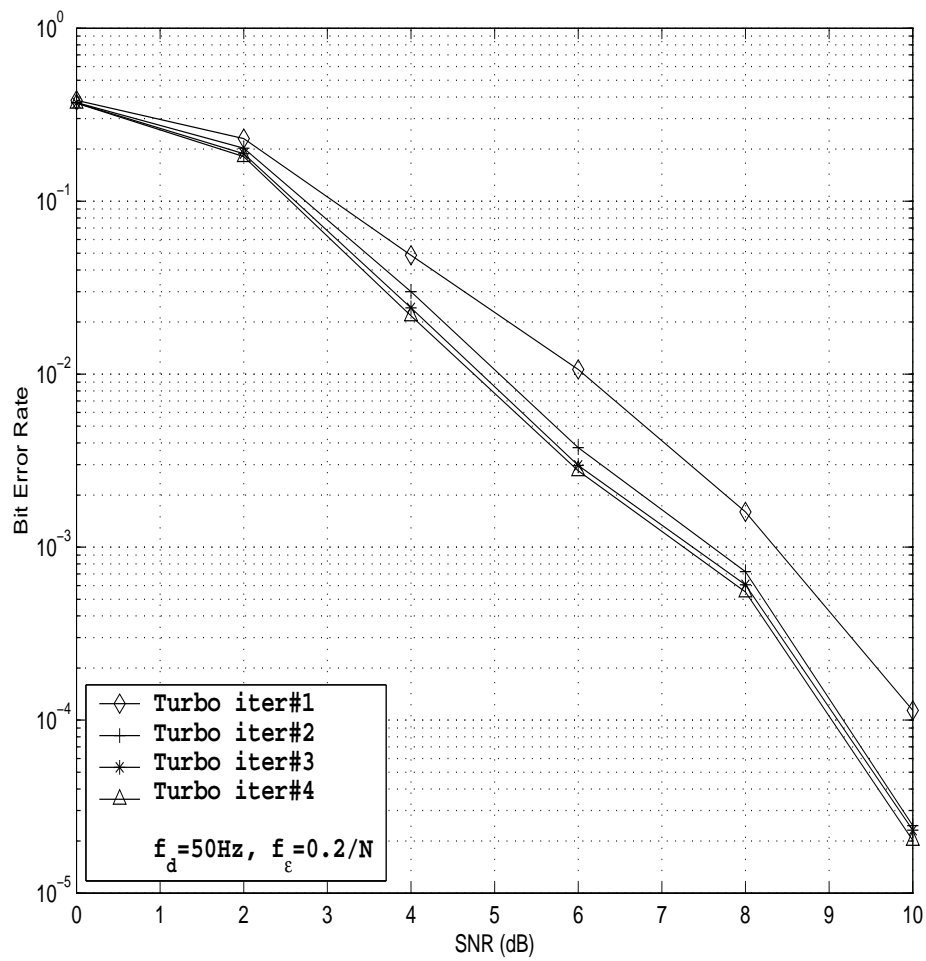


Fig. 21. BER in a coded STBC-OFDM system through a 4-tap frequency selective fading channel with Doppler shift $f_d = 50\text{Hz}$. Carrier frequency offset $f_\epsilon = 0.2/N$.

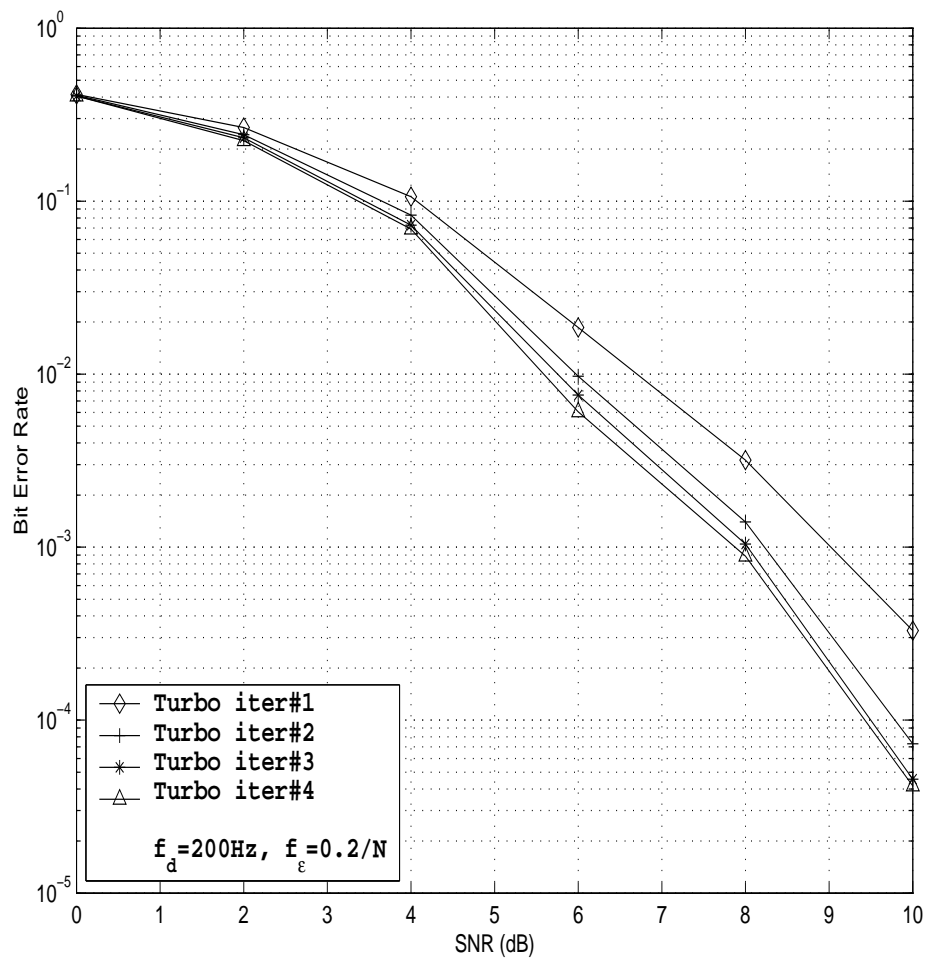


Fig. 22. BER in a coded STBC-OFDM system through a 4-tap frequency selective fading channel with Doppler shift $f_d = 200\text{Hz}$. Carrier frequency offset $f_e = 0.2/N$.

CHAPTER VI

APPLICATION OF THE PROPOSED ITERATIVE RECEIVER FOR NEW BROAD-BAND MIMO FADING CHANNEL MODEL

In this chapter, we will apply the proposed iterative receiver to STBC-OFDM systems using the physically motivated MIMO fading channel model. We will also study the effects of spatial fading correlation induced by physical parameters such as delay spread, cluster angle spread, and total angle spread.

The rest of this chapter is organized as follows. First, we introduce the broad-band MIMO fading channel model. Secondly, the fading statistics will be given in terms of delay spread, angle spread, and path gain, etc. At last, the system performance will be studied by simulations.

A. Broad-Band MIMO Fading Channel Model

In this section, we shall introduce a new model for broad-band MIMO fading channels based on a physical description of the propagation environment. Our channel model builds on previous work reported in [22], [23], [24].

1. Channel Model

We assume that the fading at the receive antennas is spatially uncorrelated. However, the spatial fading at the transmit antennas will be correlated with the correlation depending on the transmit antenna spacing and the angle spread. We model the delay spread by assuming that there are L significant scatterer clusters, which correspond to L resolvable paths, as pictured in Fig.23, and each of the paths emanating from within the same scatterer cluster experiences the same delay. Each scatterer cluster has a mean angle of arrival at the receive antenna denoted as $\bar{\theta}_l$, a cluster angle spread

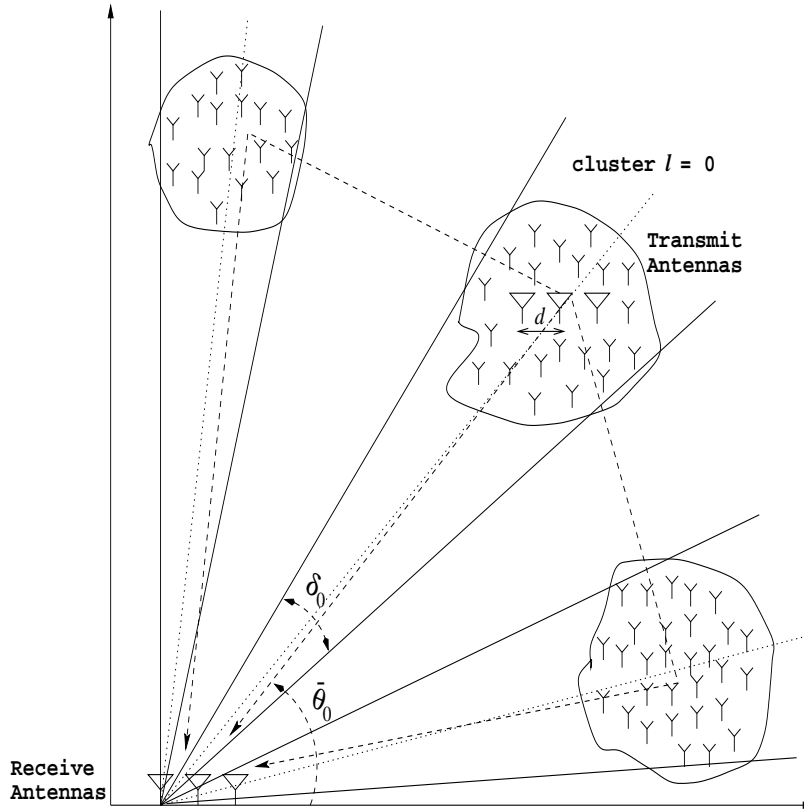


Fig. 23. Schematic representation of the MIMO delay spread channel composed of multiple clustered paths. Each path cluster has a mean angle of arrival $\bar{\theta}_l$ and an angle spread δ_l . The absolute antenna spacing is denoted by d .

δ_l , and a path gain σ_l^2 . For the sake of simplicity, we assume a uniform linear array at both the transmitter and receiver with identical antenna elements. The relative antenna spacing is denoted as $\Delta = d/\lambda$, where d is the absolute antenna spacing and $\lambda = c/f_c$ is the wavelength of a narrow-band signal with center frequency f_c . Let M_T and M_R denote the number of transmit and receive antennas, respectively, and $\underline{x}(n)$ and $\underline{y}(n)$ the discrete-time $M_T \times 1$ transmitted signal vector and $M_R \times 1$ received

signal vector, respectively, we can write:

$$\underline{y}(n) = \sum_{l=0}^{L-1} H_l \underline{x}(n-l) \quad (6.1)$$

where the $M_R \times M_T$ matrix H_l represents the l -th tap of the discrete-time MIMO fading channel impulse response. Different scatter clusters are uncorrelated, i.e.,

$$\begin{aligned} \mathbb{E}\left\{\text{vec}(H_l)\text{vec}^H(H_{l'})\right\} &= 0_{(M_T M_R \times M_T M_R)} \quad l \neq l' \\ \text{where } \text{vec}(H_l) &\triangleq [h_{l,0}, h_{l,1}, \dots, h_{l,M_R-1}]^T \\ h_{l,k} &\triangleq [h_{l,k}^{(0)}, h_{l,k}^{(1)}, \dots, h_{l,k}^{(M_T-1)}]. \end{aligned}$$

$h_{l,k}$ denotes the k -th row of the matrix H_l .

2. Fading Statistics

We assume that the $h_{l,k}$ ($l = 1, 2, \dots, L-1; k = 0, 1, \dots, M_R-1$) have zero mean and the $M_T \times M_T$ correlation matrix $R_l = \mathbb{E}\{h_{l,k}^H h_{l,k}\}$ is independent of k , or in other words, the fading statistics are the same for all receive antennas. We can write the correlation matrix R_l as follows:

$$[R_l]_{m,n} = \sigma_l^2 \rho_l((n-m)\Delta, \bar{\theta}_l, \delta_l) \quad (6.2)$$

$$\text{where } \rho_l(s\Delta, \bar{\theta}_l, \delta_l) \triangleq \mathbb{E}\left\{h_{l,k}^{(r)}(h_{l,k}^{(r+s)})^*\right\} \quad l = 0, 1, \dots, L-1. \quad (6.3)$$

Assuming that the angle of arrival for the l -th path cluster θ_l is Gaussian distributed, i.e., $\theta_l \sim \mathcal{N}(\bar{\theta}_l, \sigma_{\theta_l}^2)$, where $\sigma_{\theta_l}^2$ is proportional to the cluster angle spread δ_l , it's shown in [23] that the correlation function can be approximated for small angle spread as follows,

$$\rho_l(s\Delta, \bar{\theta}_l, \delta_l) \approx \exp\{-j2\pi s\Delta \cos(\bar{\theta}_l) - \frac{1}{2}[2\pi s\Delta \sin(\bar{\theta}_l)\sigma_{\theta_l}]^2\}. \quad (6.4)$$

Next we show how to generate H_l for our use in simulation. Recall in our previous work, we generate totally $M_T \times M_R \times L$ independent fading processes in the time domain. Now such fading processes of the same path l ($l = 1, 2, \dots, L$), to the same receiver k ($k = 1, 2, \dots, M_R$), but from different transmitters are grouped together. Thus for the time instant n , we have an $M_R \times M_T$ matrix

$$\mathbf{h}_l(n) \triangleq \begin{pmatrix} \mathbf{h}_{l,0}^{(0)}(n) & \mathbf{h}_{l,0}^{(1)}(n) & \cdots & \mathbf{h}_{l,0}^{(M_T-1)}(n) \\ \mathbf{h}_{l,1}^{(0)}(n) & \mathbf{h}_{l,1}^{(1)}(n) & \cdots & \mathbf{h}_{l,1}^{(M_T-1)}(n) \\ \vdots & \vdots & \ddots & \vdots \\ \mathbf{h}_{l,M_R-1}^{(0)}(n) & \mathbf{h}_{l,M_R-1}^{(1)}(n) & \cdots & \mathbf{h}_{l,M_R-1}^{(M_T-1)}(n) \end{pmatrix}$$

Factoring the $M_T \times M_T$ correlation matrix R_l according to $R_l = R_l^{1/2} R_l^{1/2}$, where $R_l^{1/2} \triangleq U \Lambda^{1/2} U^H$, Λ is a diagonal matrix of eigenvalues of R_l , and U is a full matrix whose columns are the corresponding eigenvectors so that $R_l \cdot U = U \cdot \Lambda$, the $M_R \times M_T$ matrix H_l for time instant n can be written as

$$H_l = \mathbf{h}_l(n) \cdot R_l^{1/2}, \quad l = 0, 1, \dots, L - 1. \quad (6.5)$$

B. Simulation Results

In this section, we provide some simulation results to illustrate the performance of the proposed iterative receiver (described in Chapter V) for STBC-OFDM system with outer channel code, using the channel model described above, with or without carrier frequency offset. In the following simulations, QPSK modulation is adopted. A rate 1/2 constraint length $\nu = 5$ convolutional code (with generators [23, 35] in octal notation) is employed as the channel code. The available bandwidth is 800kHz and is divided into 128 sub-carriers. The last eight sub-carriers are used as guard tones and the rest (120 tones) are used to transmit data. This corresponds to an OFDM

word duration of $160\mu\text{s}$. In each OFDM word, an additional guard interval of $40\mu\text{s}$ is added to combat with ISI due to the multi-path delay spread, hence the system has a total block length $T_f = 200\mu\text{s}$ and a sub-carrier symbol rate $R_b = 5\text{kHz}$. Simulations are carried out through the new channel model described by physical parameters such as cluster angle spread, mean angle spread, antenna spacing, Doppler shift, etc. The relative antenna spacing is set to $\Delta = 0.5$. The number of resolvable taps is set to $L = 4$, while the l -th elements in $\bar{\theta} = [\pi/20, \pi/10, 3\pi/20, \pi/5]$ represents the mean angle spread of the l -th tap. Hence the total angle spread is 90 degrees. The cluster angle spread σ_{θ_l} is set to be 0, 0.25 (for all $l = 0, 1, \dots, L - 1$), respectively, to implement high channel correlation to low channel correlation. For all the simulations, two transmitter antennas and one receiver antenna are used; and the \mathcal{G}_1 STBC is adopted. The OFDM system transmits in a burst manner, i.e., each data burst includes 11 OFDM words, the first OFDM word contains optimal training symbols and the rest 10 OFDM words contain 5 STBC code words. In the following figures, 24–33, the performance is demonstrated in terms of bit-error-rate (BER) versus signal to noise ratio (SNR).

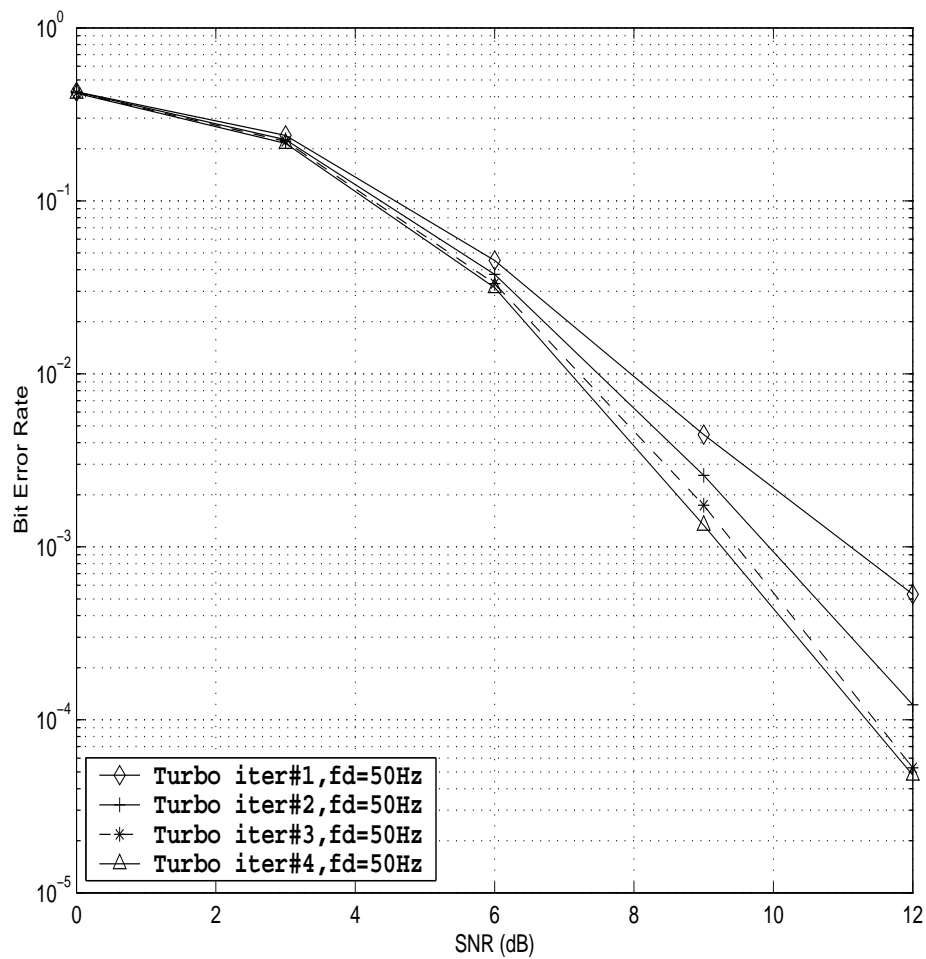


Fig. 24. A coded STBC-OFDM system through broad-band correlated MIMO channels. We assumed a total angle spread of 90 degrees and the cluster angle spread $\sigma_{\theta_l} = 0$ ($l = 0, 1, \dots, 3$). Doppler shift $f_d = 50\text{Hz}$.

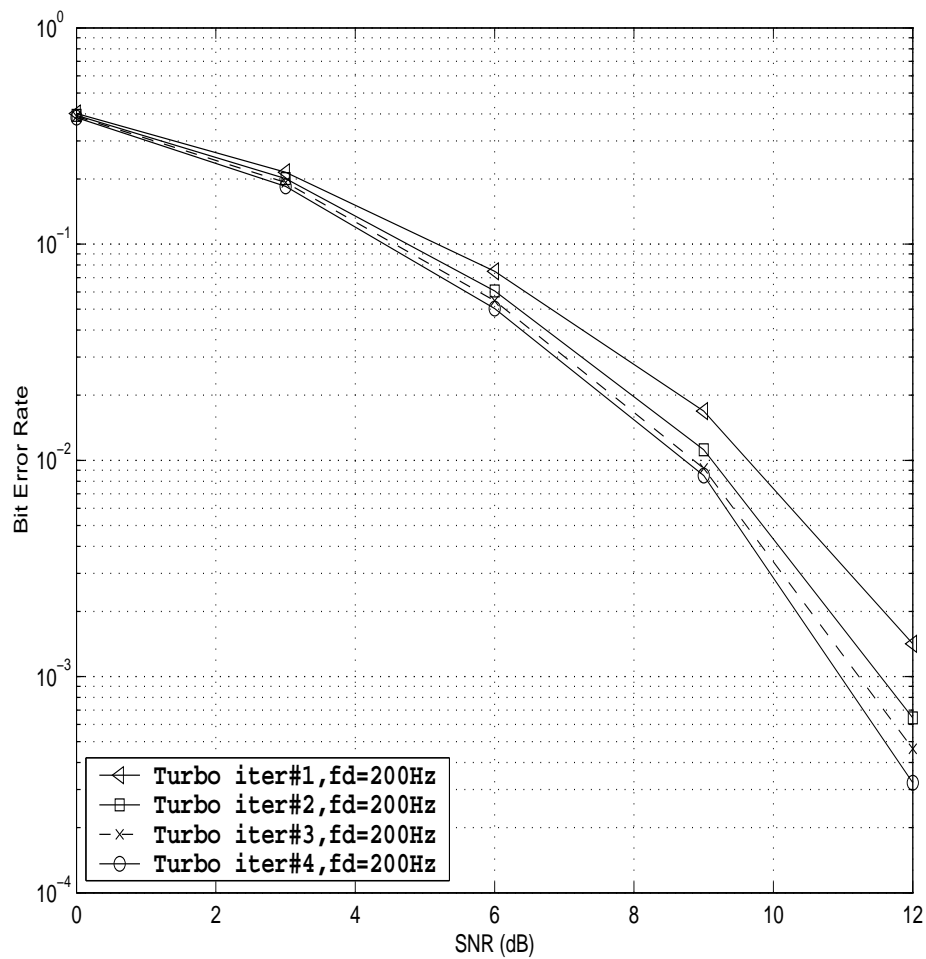


Fig. 25. A coded STBC-OFDM system through broad-band correlated MIMO channels. Doppler shift $f_d = 200\text{Hz}$. We assumed a total angle spread of 90 degrees and the cluster angle spread $\sigma_{\theta_l} = 0$ ($l = 0, 1, \dots, 3$).

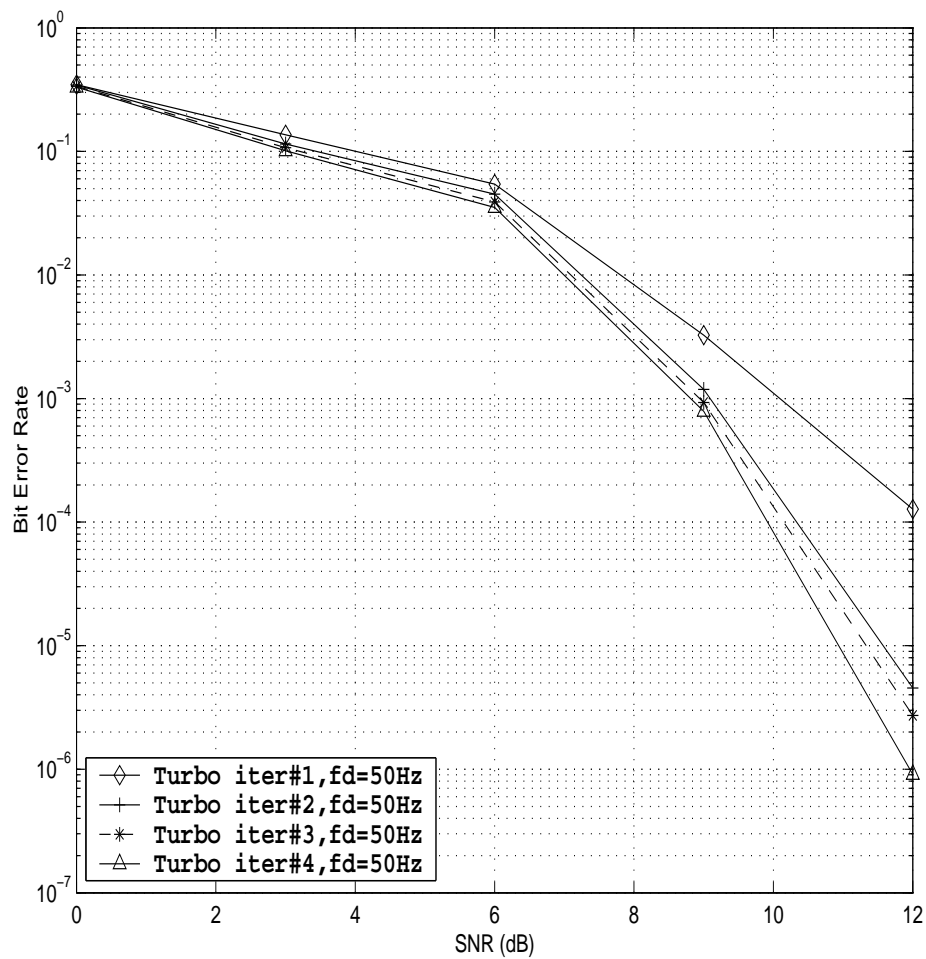


Fig. 26. A coded STBC-OFDM system through broad-band correlated MIMO channels. We assumed a total angle spread of 90 degrees and the cluster angle spread $\sigma_{\theta_l} = 0.25$ ($l = 0, 1, \dots, 3$). Doppler shift $f_d = 50\text{Hz}$.

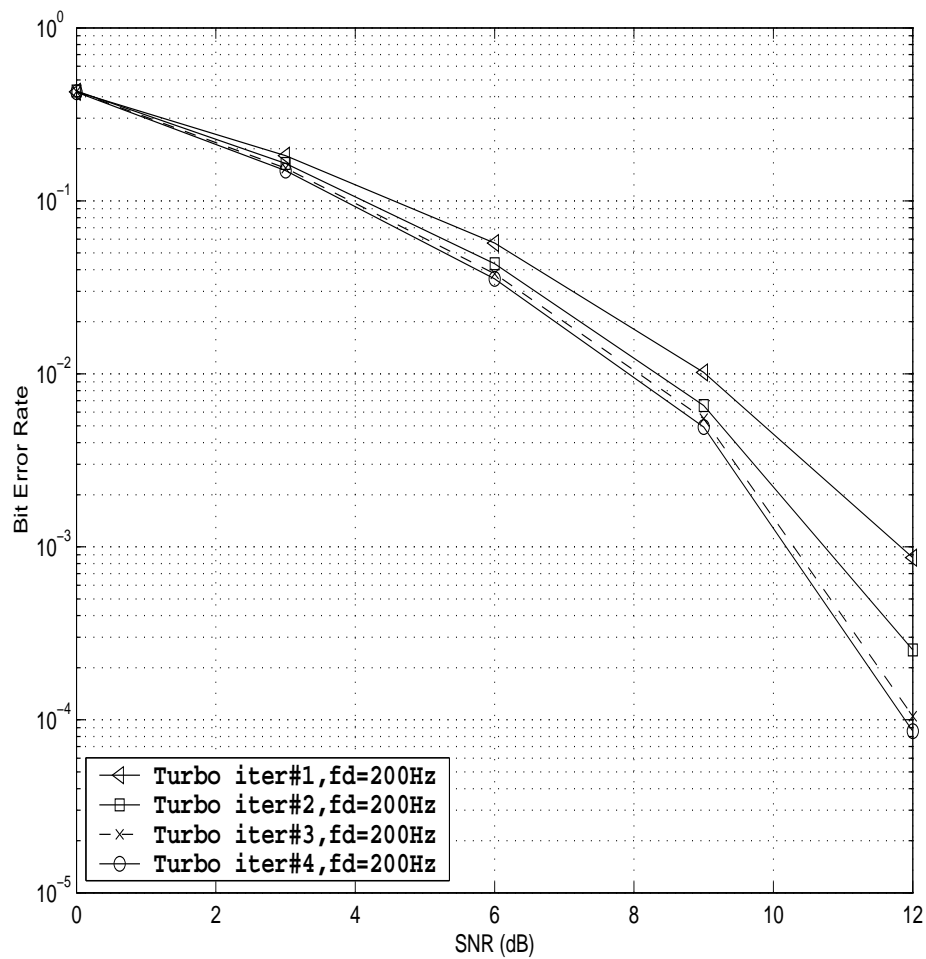


Fig. 27. A coded STBC-OFDM system through broad-band correlated MIMO channels. We assumed a total angle spread of 90 degrees and the cluster angle spread $\sigma_{\theta_l} = 0.25$ ($l = 0, 1, \dots, 3$). Doppler shift $f_d = 200\text{Hz}$.

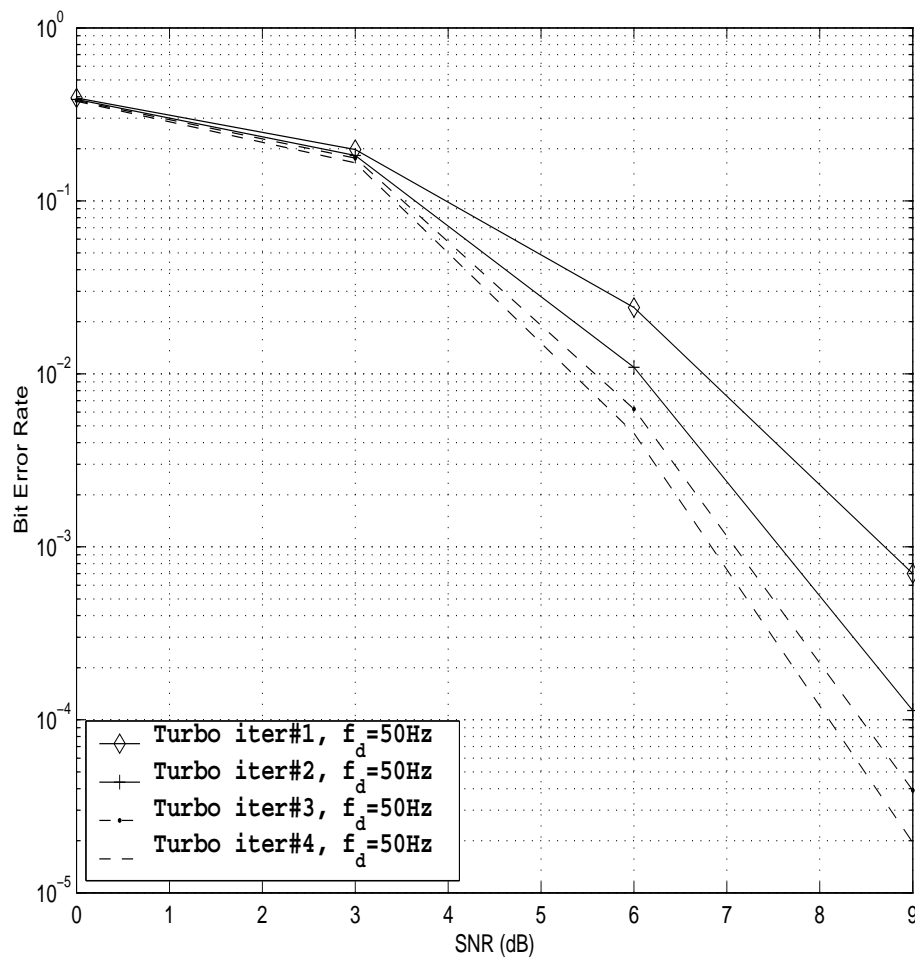


Fig. 28. A coded STBC-OFDM system through broad-band correlated MIMO channels. We assumed a total angle spread of 90 degrees and the cluster angle spread $\sigma_{\theta_l} = 1$ ($l = 0, 1, \dots, 3$). Doppler shift $f_d = 50\text{Hz}$.

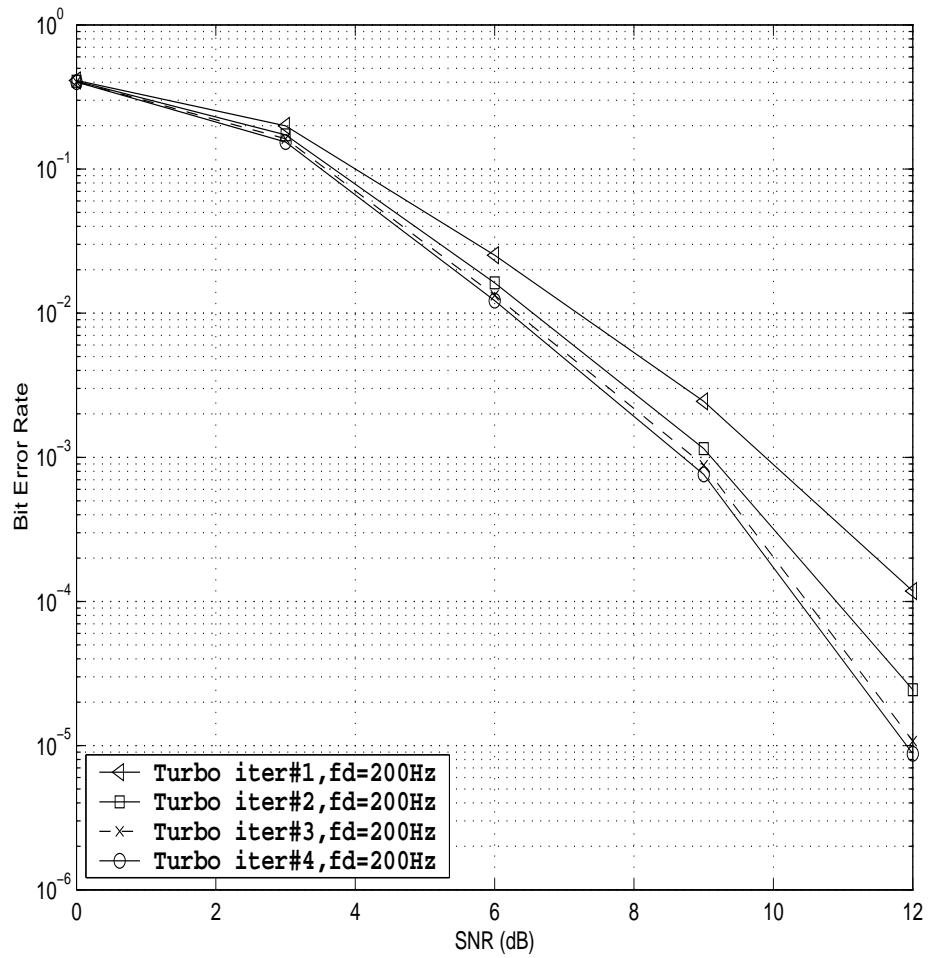


Fig. 29. A coded STBC-OFDM system through broad-band correlated MIMO channels. We assumed a total angle spread of 90 degrees and the cluster angle spread $\sigma_{\theta_l} = 1$ ($l = 0, 1, \dots, 3$). Doppler shift $f_d = 200\text{Hz}$.

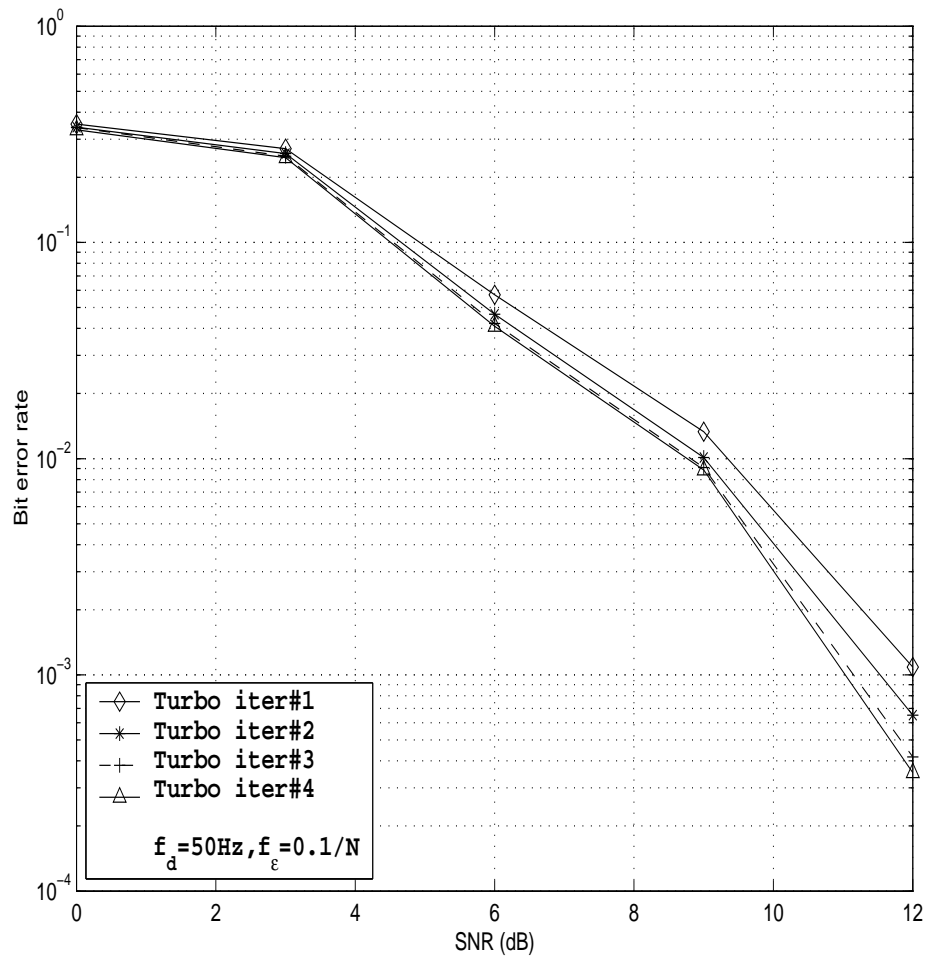


Fig. 30. A coded STBC-OFDM system through broad-band correlated MIMO channels. We assumed a total angle spread of 90 degrees and the cluster angle spread $\sigma_{\theta_l} = 0$ ($l = 0, 1, \dots, 3$). Doppler shift $f_d = 50\text{Hz}$. Frequency offset $f_\epsilon = 0.1/N$.

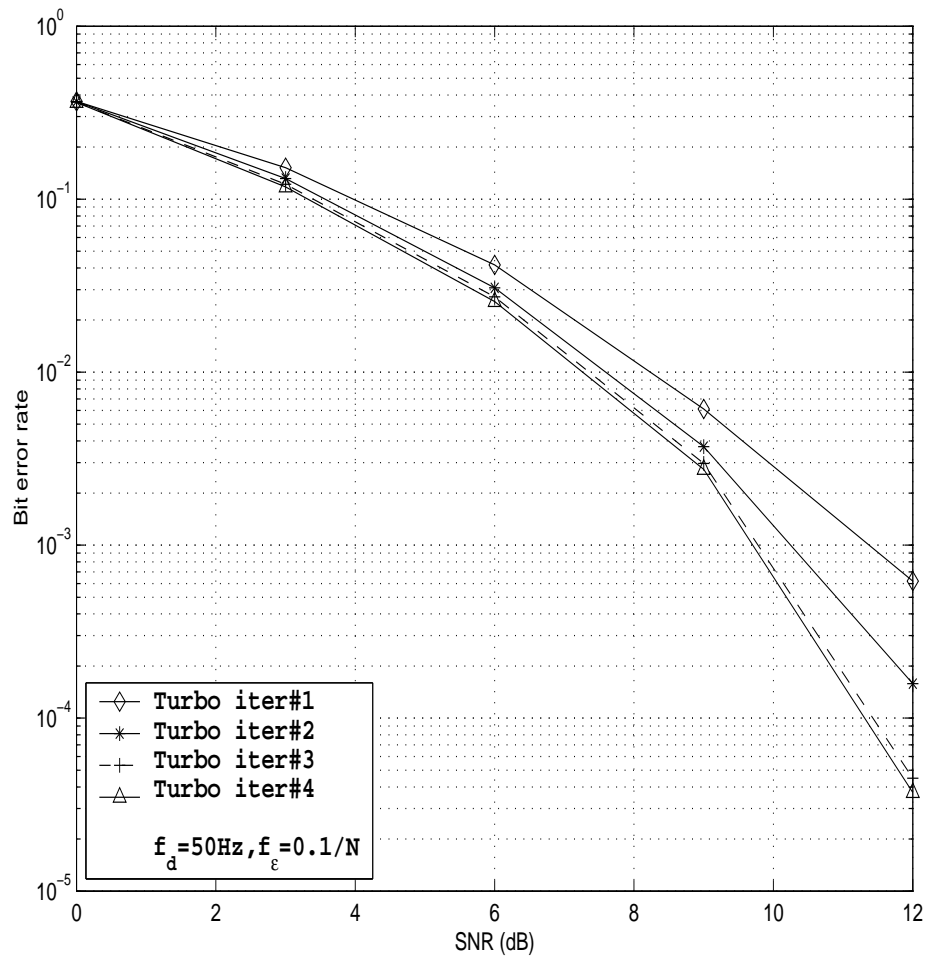


Fig. 31. A coded STBC-OFDM system through broad-band correlated MIMO channels. We assumed a total angle spread of 90 degrees and the cluster angle spread $\sigma_{\theta_l} = 0.25$ ($l = 0, 1, \dots, 3$). Doppler shift $f_d = 50\text{Hz}$. Frequency offset $f_\epsilon = 0.1/N$.

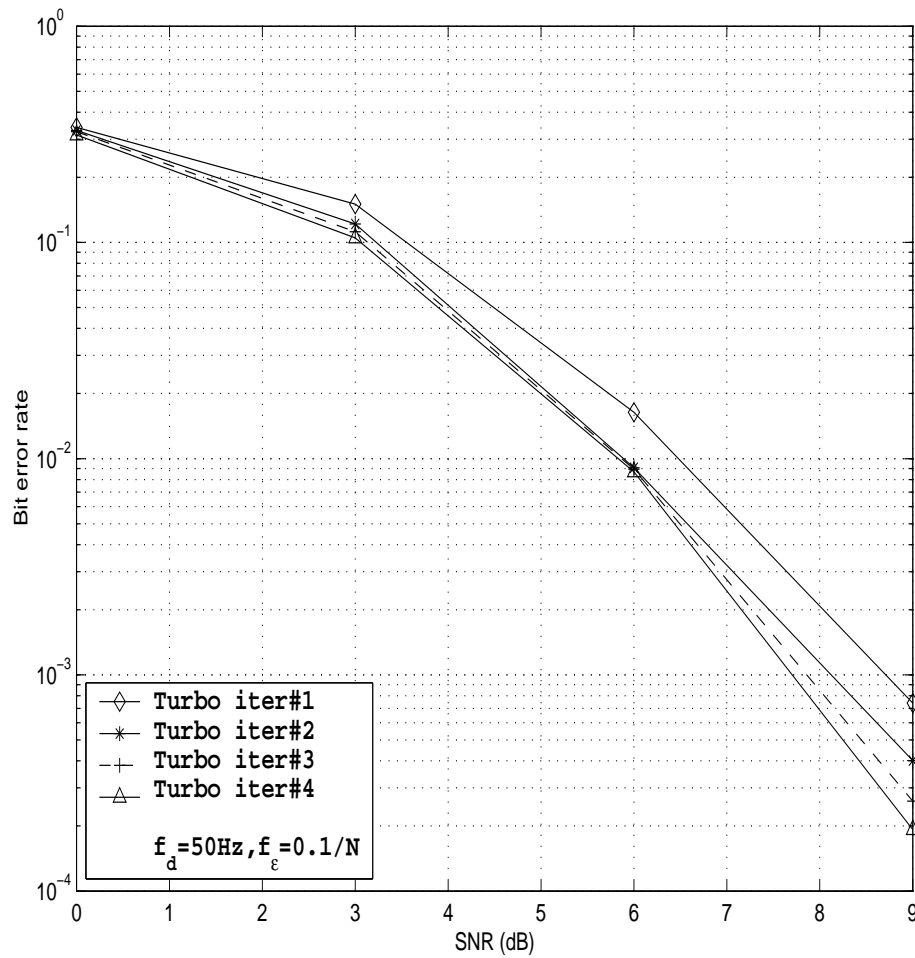


Fig. 32. A coded STBC-OFDM system through broad-band correlated MIMO channels. We assumed a total angle spread of 90 degrees and the cluster angle spread $\sigma_{\theta_l} = 1$ ($l = 0, 1, \dots, 3$). Doppler shift $f_d = 50\text{Hz}$. Frequency offset $f_\epsilon = 0.1/N$.

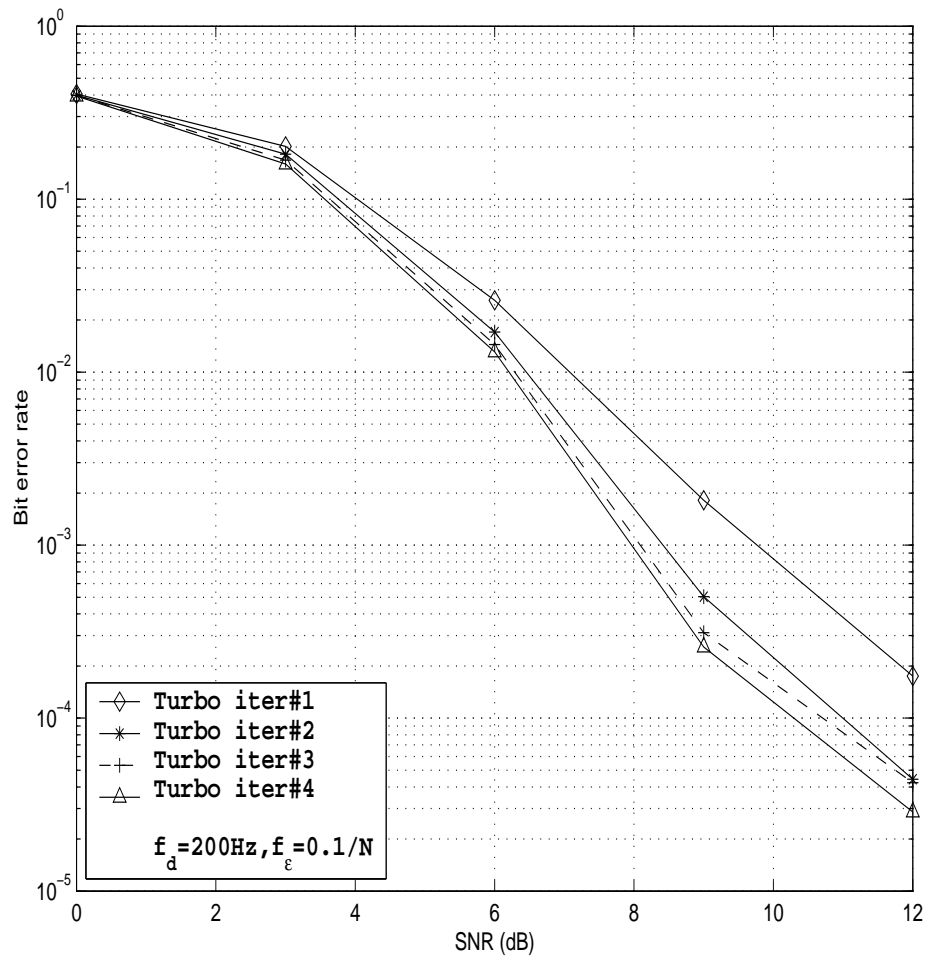


Fig. 33. A coded STBC-OFDM system through broad-band correlated MIMO channels. We assumed a total angle spread of 90 degrees and the cluster angle spread $\sigma_{\theta_l} = 1$ ($l = 0, 1, \dots, 3$). Doppler shift $f_d = 200\text{Hz}$. Frequency offset $f_\epsilon = 0.1/N$.

CHAPTER VII

CONCLUSIONS

An iterative receiver was designed for single antenna OFDM system with frequency offset and dispersive fading. The proposed receiver combined Turbo techniques and EM algorithm, and proved to be able to successively improve receiver performance by iterations. The algorithm for estimating carrier frequency offset combined the conditional maximum likelihood approach and the low-rank property of the narrow-band sub-channels. It also took advantage of available multiple frames of received data to refine the estimation. Further work was then extended to STBC-OFDM system based on similar algorithms. By introducing transmit diversity, system performance was further improved. At last, the technique was applied to STBC-OFDM system through a newly built MIMO channel model, which was based on a physical description of the propagation environment. The channels were assumed to be correlated at the transmitter end in this new model. The simulation results were satisfactory although it showed some performance degradation due to the correlation among the transmit antennas. The performance of iterative receivers for all the systems mentioned above were verified by computer simulations. Simulation results showed that the iterative techniques worked well in OFDM systems at a reasonable computational complexity.

REFERENCES

- [1] P. H. Moose, "A technique for orthogonal frequency division multiplexing frequency offset correction," *IEEE Trans. Commun.*, vol. 42, pp. 2908–2914, Oct. 1994.
- [2] M. Luise and R. Reggiannini, "Carrier frequency acquisition and tracking for OFDM systems," *IEEE Trans. Commun.*, vol. 44, pp. 1590–1598, Nov. 1996.
- [3] F. Daffara and A. Chouly, "Maximum likelihood frequency detectors for orthogonal multicarrier systems," in *Proc. IEEE Int. Conf. Commun.*, Geneva, Switzerland, pp. 766–771, May. 1993.
- [4] F. Daffara and O. Adami, "A new frequency detector for orthogonal multicarrier transmission techniques," in *Proc. IEEE Veh. Technol. Conf.*, Chicago, IL, pp. 804–809, Jul. 1995.
- [5] H. Ge and K. Wang, "Efficient method for carrier offset correction in OFDM system," in *Proc. IEEE ICASSP*, vol. 5, pp. 2467–2470, 1999.
- [6] X. Wang and H. Poor, "Iterative (Turbo) soft interference cancelation and decoding for coded CDMA," *IEEE Trans. Commun.*, vol. 47, pp. 1046–1061, Jul. 1999.
- [7] T. S. Rappaport, *Wireless Communications: Principles and Practice*. Upper Saddle River, NJ: Prentice Hall PTR, 1996.
- [8] B. Lu and X. Wang, "Iterative receivers for multiuser space-time coding systems," *IEEE J. Select. Areas Commun.*, vol. 18, pp. 2322–2335, Nov. 2000.

- [9] H. V. Poor, *An Introduction to Signal Detection and Estimation*, New York: Springer-Verlag, 1988.
- [10] B. Lu and X. Wang, "Bayesian blind turbo receiver for coded OFDM systems with frequency offset and frequency-selective fading," *IEEE J. Select. Areas Commun.*, vol. 19, pp. 2516–2527, Dec. 2001.
- [11] B. Lu, X. Wang and Y. Li, "Iterative receivers for space-time block coded OFDM systems in dispersive fading channels," *IEEE Trans. Wireless Commun.*, vol. 1, pp. 213–225, Apr. 2002.
- [12] M. Uysal, N. Al-Dhahir, and C. N. Georghiades, "A space-time block-coded OFDM scheme for unknown frequency-selective fading channels," *IEEE Commun. Lett.*, vol. 5, pp. 393–395, Oct. 2001
- [13] R. A. Stirling-Gallacher and Z. Wang, "Improving performance of coherent coded OFDM systems using space time transmit diversity," *Electron. Lett.*, vol. 37, pp. 457–458, Mar. 2001
- [14] S. M. Alamouti, "A simple transmit diversity technique for wireless communications," *IEEE J. Select. Areas Commun.*, vol. 16, pp. 1451–1458, Oct. 1998.
- [15] V. Tarokh, H. Jafarkhani and A. R. Calderbank, "Space-time block coding for wireless communications: performance results," *IEEE J. Select. Areas Commun.*, vol. 17, pp. 451–460, Mar. 1999.
- [16] S. Kung, Y. Wu and X. Zhang, "Bezout space-time precoders and equalizers for MIMO channels," *IEEE Trans. Signal Processing*, vol. 50, pp. 2499–2514, Oct. 2002

- [17] V. Tarokh, A. Naguib, N. Seshadri and A. R. Calderbank, "Space-time codes for high data rate wireless communication: performance criteria in the presence of channel estimation errors, mobility, and multiple paths," *IEEE Trans. Commun.*, vol. 47, pp. 199–207, Feb. 1999
- [18] G. J. McLachlan and T. Krishnan, *The EM Algorithm and Extensions*, New York: John Wiley & Sons Inc, 1997.
- [19] X. Ma, H. Kobayashi and S. C. Schwartz, "EM-based channel estimation for OFDM," in *IEEE Pacific Rim Conf. Commun., Computers and Signal Processing*, vol. 2, pp. 449–452, 2001.
- [20] Y. Li, L. J. Cimini, Jr. and N. R. Sollenberger, "Robust channel estimation for OFDM systems with rapid dispersive fading channels," *IEEE Trans. Commun.*, vol. 46, pp. 902–915, Jul. 1998.
- [21] C. N. Georghiades and J. Han, "Sequence estimation in the presence of random parameters via the EM algorithm," *IEEE Trans. Commun.*, vol. 45, pp. 300–308, Mar. 1997.
- [22] H. Bolckei, D. Gesbert and A. J. Paulraj, "On the capacity of OFDM-based spatial multiplexing systems," *IEEE Trans. Commun.*, vol. 50, pp. 225–234, Feb. 2002.
- [23] D. Asztely, "On antenna arrays in mobile communication systems: fast fading and GSM base station receiver algorithms," Royal Institute of Technology, Stockholm, Sweden, IR-S3-SB-9611, 1996.
- [24] J. Fuhl, A. F. Molisch and E. Bonek, "Unified channel model for mobile radio systems with smart antennas," in *Proc. Inst. Elect. Eng.*, vol. 145, pp. 32–41,

Feb. 1998.

VITA

Hui Liu was born in Beijing, China. Her permanent address is: Computer Institute 7-4, No.56 Xisanhua North Road, Haidian District, Beijing 100044, P.R.China. She graduated from Tsinghua University in 2000 with a B.S in electrical engineering. From September 2000 to May 2003, she studied at Texas A&M University for her M.S. degree.

The typist for this thesis was Hui Liu.